
Uniwersytet
Gdański

Faculty of Biology

University of Gdańsk

Soroosh Monem

Formation of protein aggregates and glycation products in *Escherichia coli* and *Klebsiella pneumoniae* exposed to desiccation-rehydration stress

PhD thesis presented to The Scientific Council of Biological Sciences of the University of Gdańsk in order to obtain a doctoral degree in the field of exact and natural sciences in the discipline of biological sciences

Supervisor: **Prof. Dr. hab. Ewa Laskowska**

Faculty of General and Medical Biochemistry

GDAŃSK 2026

Wydział Biologii

Uniwersytet Gdański

Mgr Soroosh Monem

Powstawanie agregatów białek i produktów glikacji u *Escherichia coli* i *Klebsiella pneumoniae* narażonych na stres związany z wysuszaniem-rehydratacją

Praca przedstawiona
Radzie Dyscypliny Nauki biologiczne Uniwersytetu Gdańskiego
celem uzyskania stopnia doktora
w dziedzinie nauk ścisłych i przyrodniczych
w dyscyplinie nauki biologiczne

Promotor: Prof. dr hab. Ewa Laskowska

Katedra Biochemii Ogólnej i Medycznej

GDAŃSK 2026

The study on *K. pneumoniae* was conducted as part of the NCN project 2018/29/Z/NZ6/01040, "„Fighting antibiotic-resistant superbugs with anti-persister compounds targeting the stringent response” (Joint Programming Initiative on Antimicrobial Resistance JPI EC AMR Call 2018)

Dedication

تقدیم بہ عبدالرزاق، پدر صبور،
شہرزاد، (نیکوی کوچک) ،
برای تمام ایام سالہا

Acknowledgements

I extend my sincere gratitude to Professor Ewa Laskowska, whose dedicated mentorship and expert guidance over the past six years have been pivotal to the completion of this thesis. Their profound insights and steadfast support have profoundly shaped my research journey.

I also thank Professor Dorota Kuczyńska-Wiśnik for their intermittent assistance and thoughtful contributions, which provided valuable perspectives at key moments.

Furthermore, I acknowledge Dr. Karolina Stojowska-Swędrzyńska for their availability in the laboratory, offering helpful responses to inquiries and general support as needed.

Abstract

In natural environments, bacteria often enter an anhydrobiotic state due to water loss. Desiccation results in molecular condensation and membrane disruption. Reduction of the hydration shell around proteins causes their inactivation, unfolding, and aggregation. The loss of protein stability and increased molecular crowding favor harmful reactions, including non-enzymatic glycosylation (glycation or the Maillard reaction), which leads to irreversible cross-linking of macromolecules and the accumulation of advanced glycation end-products (AGEs). Preliminary studies demonstrated that although glycation may induce protein aggregation *in vitro*, aggregates formed in *Escherichia coli* exposed to desiccation contained relatively low levels of AGEs compared to the soluble protein fraction.

Protein aggregation in bacteria caused by various intrinsic or environmental stresses disrupts proteostasis and exerts detrimental effects, including loss of protein function, nonspecific interactions with macromolecules, sequestration of functional proteins, and membrane damage. Recent studies have demonstrated that under specific conditions protein aggregates in bacteria play protective roles as functional compartments. Preliminary experiments suggested that glycation, rather than protein aggregation, is the main cause of *E. coli* death under desiccation stress.

The aim of this work was to verify this hypothesis and extend the study of stress-induced protein aggregation and glycation in *E. coli* and *Klebsiella pneumoniae*. The influence of osmolytes (carnosine, glycine-betaine, and trehalose) on bacterial viability, protein aggregation and glycation was investigated. It was found that protein aggregation was inhibited or enhanced depending on the osmolyte and its concentration used. Lower concentrations of carnosine, betaine, and trehalose inhibited the formation of protein aggregates and glycation products, thereby increasing *E. coli* viability under desiccation-rehydration stress. Although high concentrations of betaine and trehalose significantly enhanced protein aggregation, glycation was still inhibited and *E. coli* cells survived desiccation stress better than bacteria grown without osmolytes. Independent of concentration, all osmolytes caused enhanced protein aggregation and increased viability of *K. pneumonia* MKP103. Therefore, these results confirmed that glycation rather than protein aggregation is the main cause of cell death upon desiccation stress.

Further experiments showed that in *E. coli*, Nε-lysine acetylation may prevent the formation of carboxymethyl-lysine (CML), a non-fluorescent AGE product, thereby improving bacterial survival under desiccation-rehydration stress. The OmpC porin was identified as one of the most glycated proteins in *E. coli.*

The relationship between cell viability, protein aggregation, and glycation was also investigated using macrocolonies of the *K. pneumoniae* clinical isolate 577-BA. The macrocolonies formed two subpopulations: a mucoid/capsular center and a non-

mucoid/non-capsular ring. The comparison of the center and ring genomes revealed that the appearance of the non-mucoid/non-capsular ring subpopulation resulted from the disruption of the *wbaP* gene by Insertion Sequence (IS)5 insertion. The *wbaP* gene encodes undecaprenyl-phosphate galactose phosphotransferase, an enzyme catalyzing the first step of capsule production. The loss of capsule was advantageous for the ring subpopulation, as it facilitated biofilm formation. The ring subpopulation was characterized by higher viability, lower levels of AGEs, and greater protein aggregation than the center subpopulation. Taken together, these results confirmed that the primary cause of bacterial viability loss during stress is glycation, not protein aggregation, suggesting that aggregates may have protective functions.

Streszczenie

W środowisku naturalnym bakterie często przechodzą w stan anhydrobiozy z powodu utraty wody. Wysuszanie powoduje zagęszczenie makrocząsteczek i rozerwanie błony komórkowej. Redukcja otoczki hydratacyjnej wokół białek powoduje ich inaktywację, rozfałdowanie i agregację. Utrata stabilności białek i zagęszczenie sprzyjają szkodliwym reakcjom, w tym nieenzymatycznej glikozylacji (glikacji lub reakcji Maillarda), która prowadzi do nieodwracalnego sieciowania makrocząsteczek i gromadzenia zaawansowanych produktów glikacji (AGEs). Wstępne badania wykazały, że chociaż glikacja może indukować agregację białek *in vitro*, agregaty powstające w komórkach *Escherichia coli* narażonych na wysuszanie zawierały stosunkowo niski poziom AGEs w porównaniu z rozpuszczalną frakcją białkową.

Agregacja białek u bakterii wywołana różnymi czynnikami wewnętrznymi lub stresem środowiskowym prowadzi do zaburzenia proteostazy i wywołuje szkodliwe skutki: utratę funkcji, niespecyficzne oddziaływanie z makrocząsteczkami, sekwestrację białek funkcjonalnych i uszkodzenie błony komórkowej. Ostatnie badania wykazały, że w określonych warunkach bakteryjne agregaty białkowe mogą pełnić rolę ochronną jako funkcjonalne kompartmenty. Wstępne doświadczenia sugerowały, że to glikacja, a nie agregacja białek, jest główną przyczyną śmierci *E. coli* podczas wysuszania.

Celem niniejszej pracy była weryfikacja tej hipotezy i rozszerzenie badań nad agregacją i glikacją białek indukowaną stresem u *E. coli i Klebsiella pneumoniae*. Zbadano między innymi wpływ osmolitów (karnozyny, glicyny-betainy i trehalozy) na żywotność bakterii, agregację i glikację białek. Stwierdzono, że agregacja białek była hamowana lub indukowana w zależności od zastosowanego osmolitu i jego stężenia. Niższe stężenia karnozyny, betainy i trehalozy hamowały tworzenie agregatów białkowych i produktów glikacji, zwiększając tym samym przeżywalność *E. coli* podczas stresu związanego z wysuszeniem i rehydratacją. Chociaż wysokie stężenia betainy i trehalozy znacząco zwiększały agregację białek, glikacja była nadal hamowana, a komórki *E. coli* przetrwały stres związany z wysuszaniem lepiej niż bakterie hodowane bez osmolitów. Niezależnie od stężenia, wszystkie osmolity powodowały wzmożoną agregację białek i podwyższały żywotność *K. pneumoniae* MKP103. Zatem wyniki te potwierdziły, że to glikacja, a nie agregacja białek, jest główną przyczyną śmierci bakterii podczas wysuszania.

Dalsze doświadczenia wykazały, że u *E. coli* acetylacja Nε-lizyny może zapobiegać tworzeniu karboksymetylolizyny (CML), niefluorescencyjnego produktu AGE, zwiększając w ten sposób przeżywalność bakterii podczas wysuszania i rehydratacji. Jako jedno z najsilniej glikowanych białek w *E. coli* zidentyfikowano porynę OmpC.

Zbadano również związek między przeżywalnością komórek, agregacją białek i glikacją, wykorzystując makrokolonie klinicznego izolatu *K. pneumoniae* 577-BA. Makrokolonie tworzyły dwie subpopulacje: mukoidalne centrum z otoczką i niemukoidalny/bezotoczkowy pierścień. Porównanie genomów centrum i pierścienia wykazało, że pojawienie się niemukoidalnej subpopulacji wynikało z przerwania genu *wbaP* przez insercję IS5. Gen *wbaP* koduje enzym katalizujący pierwszy etap syntezy otoczki, fosfotransferazę undekaprenylofosforanu galaktozy. Utrata otoczki była korzystna dla subpopulacji pierścienia, ponieważ umożliwiała tworzenie biofilmu. Subpopulacja pierścienia charakteryzowała się wyższą żywotnością, niższym poziomem AGEs i zwiększoną agregacją białek niż centrum makrokolonii. Podsumowując, wyniki te potwierdziły, że główną przyczyną utraty żywotności bakterii podczas stresu jest glikacja, a nie agregacja białek, co sugeruje, że agregaty mogą pełnić funkcje ochronne.

Table of Contents

List of Figures

List of Tables

Abbreviations and Acronyms

AcK	**Ac**etyl Lysine (**K**)
AcP	**ac**etyl**p**hosphate
AGEs	**A**dvanced **G**lycation **E**nd-products
APRs	**a**ggregation-**p**rone **r**egions
APS	**a**mmonium **p**er**s**ulfate
ATP	**a**denosine **t**ri**p**hosphate
Aβ	**A**myloid **beta**
bcsA	**B**acterial **c**ellulose **s**ynthase subunit **A**
CFU/mL	**c**olony-**f**orming **u**nits per **m**illi**l**iter
CML	**C**arboxy**m**ethyl **L**ysine
CobB	NAD-dependent protein-lysine deacetylase
CPS	**c**apsular **p**olysaccharide **s**ynthesis
CsgA	**C**urli **s**pecific **g**ene **A**
DNP	**Di**nitro**p**henyl
DNPH	2,4-**di**nitro**p**henyl**h**ydrazine
DPs	**D**NA-binding **p**rotein from **s**tarved cells
DTT	**di**thio**t**hreitol
EF-Tu	**E**longation **f**actor **t**hermo **u**nstable
entA-F	**Ent**erobactin biosynthesis proteins **A** through **F**
EnvZ/OmpR	**Env**ironmental **Z** sensor and **O**uter **m**embrane **p**orin **R**egulator
ESBL	**E**xtended-**s**pectrum **β**-**l**actamase
FASTA, fast A	**Fast**-**A**ll
fimH	Type 1 **fim**brial adhesin subunit **H**
GrcA	**A**utonomous **g**lycyl **r**adical **c**ofactor
GroEL/ES	**Gro**wth operon in ***E. coli*** **l**arger protein (***E. coli*** **s**maller protein)
HRP	**h**orse **r**addish **p**eroxidase
HutU/HutH	Urocanate hydratase (HutU) and histidine ammonia-lyase (HutH)
IDPs	**I**ntrinsically **D**isordered **P**roteins
IDR	**I**ntrinsically **D**isordered **R**egion
IS	**I**nsertion **S**equence
iutA	TonB-dependent iron uptake siderophore
KAT	Lysine (**K**)-**A**cetyl **T**ransferase
KatG	Catalase-peroxidase
kDa	**K**ilo **Da**lton
LB	**L**ysogeny **B**roth
LLPS	**l**iquid-**l**iquid **p**hase **s**eparation
LPS	**L**ipo**p**oly**s**accharide
MDA	**m**alon**di**aldehyde
MDR	**M**ulti**d**rug-**r**esistant
MGO	**M**ethyl**g**ly**o**xal

MLOs	**m**embrane-**l**ess **o**rganelles
NDM	**N**ew **D**elhi **m**etallo-β-lactamase
NGS	**N**ext **G**eneration **S**equencing
NIH	**N**ational **I**nstitutes of **H**ealth
OD	**o**ptical **d**ensity
OM	**O**uter **m**embrane
Omp	**O**uter **m**embrane **p**orin
otsAB	**O**smoregulated **t**rehalose **s**ynthesis, gene **A** and **B**
OxyR	**oxi**dative stress **r**egulator
PAA	**p**oly**a**cryl**a**mide
PBS	**P**hosphate-**b**ased **s**aline
pgaABC	**P**oly-beta-1,6-N-**a**cetyl-D-**g**lucosamine biosynthesis proteins **A**, **B**, **C**
PHPT	**p**olyisoprenyl-phosphate **h**exose-1-**p**hosphate **t**ransferases
PI	**p**ropidium **i**odide
ProU/ProP	**Pro**line **u**ptake system (ProU operon) and **Pro**line **p**ermease (ProP)
PS	**p**oly**s**tyrene
Pta	**p**hospho**t**rans**a**cetylase
PVC	**p**oly**v**inyl **c**hloride
ROS	**R**eactive **O**xygen **S**pecies
RpoS	**R**NA **po**lymerase **s**igma factor S (σ^s or σ^{38})
Rps	**R**ibosomal **p**roteins of the **s**mall (30S) subunit
SDS-PAGE	**S**odium **d**odecyl **s**ulfate **p**oly**a**crylamide **g**el **e**lectrophoresis
Ssb	**s**ingle-**s**tranded DNA-**b**inding protein
SstT	sodium-coupled Serine/threonine symporter
ST258	**s**equence **t**ype **258**
T6SS	**t**ype **VI** **s**ecretion **s**ystem
TBARS	**t**hio**b**arbituric **a**cid-**r**eactive **s**ubstances
TBS	**T**ris-**b**ased **B**uffer
TEMED	**te**tra**m**ethyl**e**thylene**d**iamine
v/v %	$\frac{Volume\ of\ solute\ (CO_2)}{Total\ volume\ of\ mixture} \times 100$
VBNC	**v**iable-**b**ut-**n**on-**c**ulturable
w/v	**w**eight per **v**olume
wbaP	Undecaprenyl-phosphate galactose phosphotransferase
WT	**W**ild **T**ype
YfiQ	lysine acetyltransferase

I. Introduction

Protein aggregates in bacteria

Protein aggregation in bacteria, caused by numerous intrinsic or environmental stresses, often leads to disruptions of proteostasis and various detrimental effects in the cell. These effects can include loss of protein function, an overload of the protein quality control systems, nonspecific interactions with macromolecules, sequestration of functional proteins, and membrane damage. In aging or heat-stressed *E. coli* cells, aggregates typically localize at older cell poles and are thereby inherited asymmetrically after division, contributing to differential daughter cell fitness (Książek, 2010; Lindner et al., 2008; Rokney et al., 2009; Winkler et al., 2010). This strategy reduces toxic effects caused by misfolded proteins and enables the whole bacterial population to withstand stressful conditions.

The increasing number of studies demonstrated that protein aggregates, besides exerting toxic effects, may serve as functional compartments in bacteria under specific conditions (Govers et al., 2018; Jin et al., 2021; Pei et al., 2025; Pu et al., 2019). The aggregates sequester misfolded proteins, protecting them from degradation or from nonspecific interactions with soluble components or membranes. Thus, the aggregates are less toxic than soluble misfolded monomers or oligomeric intermediates. Under favorable conditions, proteins may be recovered from aggregates and refolded, which requires less cellular energy than *de novo* synthesis.

Numerous studies have shown that protein aggregation in bacteria and eukaryotes is driven by liquid-liquid phase separation (LLPS) (Kuczyńska-Wiśnik et al., 2023). LLPS relies on the separation of a homogeneous macromolecular solution into dense condensates (liquid droplets) and a diluted phase. Liquid droplets are highly dynamic structures whose components may diffuse between phases. LLPS-driven protein condensates, so-called membrane-less organelles (MLOs) have been shown to be involved in multiple processes, such as replication, transcription, cell division, and stress tolerance. In bacteria, MLOs contribute to various mechanisms, including protecting proteins and RNA from irreversible inactivation or degradation, activating molecular

chaperones, and inducing a dormant state that confers antibiotic and stress tolerance. (**Table 1**).

Table 1. Examples of protective protein aggregates in bacteria

Species	Stress inducing aggregation	Protection against	Mechanism of protection	Ref.
E. coli	Sublethal heat stress, hydrogen peroxide, streptomycin	More severe heat shock	"Memory aggregates". Induction of protein quality control components	Govers et al., 2018
A. baumannii	Desiccation, streptomycin, Δ*lon* mutation	Desiccation	Protection of sequestered proteins	Wang et al., 2020
E. coli	Stationary phase	Antibiotics	Dormancy induced by aggregates	Leszczynska et al, 2013
***E. coli* and other Gram-negative bacteria**	Stationary phase, heat shock, streptomycin, hydrogen peroxide	Antibiotics	Dormancy induced by aggresomes	Jin et al., 2021; Pu et al., 2019
Salmonella typhimurium	Macrophage derived ROS	Antibiotics	Dormancy induced by aggresomes	Chen et al., 2025
E. coli	ATP-depletion due to arsenite stress	Arsenite stress	Aggresomes protect RNA against ribonucleases	Pei et al., 2025

Over time, under prolonged stress or during aging, liquid droplets can be converted into solid- like irreversible structures. In dormant bacteria, this liquid-to-solid phase transition prevents aggregate dissolution and growth resumption. In consequence, the bacteria enter the viable but non-culturable (VBNC) state (Bollen et al., 2025)

Desiccation stress and protein aggregates

The most common stress that bacteria encounter in the natural environment is desiccation. Water loss leads to the condensation of molecules and membrane

disruption. Reduction of the hydration shell around proteins causes their inactivation, denaturation and aggregation (It was found that among the 547 proteins identified in the aggregates formed in *E. coli* during desiccation-rehydration stress, the most abundant were ribosomal proteins, elongation factor EF-Tu, tryptophanase A, and Dps (Kuczyńska-Wiśnik et al., 2023). The high abundance of these proteins in the aggregates reflected their high cellular levels, but it was not the only factor triggering aggregation. Using various applications and algorithms, such as PONDR (http://www. pondr. com), Fuz- Drop (https://fuzdrop. bio. unipd. it/predictor), PSPredictor (http://www. pkumdl. cn: 8000/PSPredictor), and the DisProt database (DisProt), it was possible to identify proteins with disordered sequences or aggregation-prone regions (APRs) and tendencies toward liquid- liquid phase separation. All these features may promote the formation of liquid droplets that then transform into solid-like aggregates. Depending on the predictors, 8-16 LLPS-prone proteins, including Dps, Ssb, and ribosomal proteins, were identified. Dps is overexpressed in response to starvation and is one of the main DNA-binding proteins in the stationary phase. It was demonstrated that Dps causes condensation of nucleic acids into globular phase- separated coacervates both in vivo and in vitro (Gupta et al., 2023; Orban and Finkel, 2022). SSB is one of six *E. coli* prion-like proteins annotated in the DisProt database of experimentally confirmed intrinsically disordered proteins (IDPs). There are 121 *E. coli* IDPs in the DisProt database, of which 31 have been detected in the aggregates. Fourteen proteins with at least 60% disordered sequence were detected. Notably, most LLPS- prone proteins in the aggregates had at least 30% disordered sequence and at least one Intrinsically Disordered Region (IDR) longer than 35 amino acids. These analyses indicated that during desiccation-rehydration stress, protein aggregates in *E. coli* form via distinct pathways, including LLPS, disordered-sequence interactions, and APRs. Aggregates may be a mixture of different condensates: liquid and stable aggregates with different sets of proteins. During the transition from liquid to solid state, small condensates, oligomers, or aggregates may merge into larger ones.

Formation of Glycation Products

Advanced Glycation End-products (AGEs) are formed endogenously through non-enzymatic reactions under conditions such as hyperglycemia and oxidative stress, involving pathways like the Maillard reaction where reducing sugars condense with amine groups of proteins, lipids, or nucleic acids (Twarda-Clapa et al., 2022). Key precursors include glucose, fructose, and reactive dicarbonyls like methylglyoxal (MGO), which accelerate AGE accumulation via oxidation and rearrangement (Rungratanawanich et al., 2021). The chemical process begins with the reversible formation of Schiff bases from carbonyl groups of sugars and free amine groups, followed by irreversible Amadori rearrangements yielding early glycation products (Twarda-Clapa et al., 2022). Further oxidation, dehydration, and fragmentation produce reactive intermediates like glyoxal and MGO, which form stable cross-links through Michael addition or additional condensations (Perrone et al., 2020). Lipid peroxidation contributes to related advanced lipoxidation end-products, enhancing the heterogeneity of AGE structures (Fu et al., 1996). AGEs are classified by origin as endogenous or exogenous, with endogenous types arising from metabolic pathways and exogenous from diet or environmental sources (Twarda-Clapa et al., 2022). Based on chemical structure and properties, they include fluorescent cross-linking types like pentosidine and non-fluorescent non-cross-linking types such as carboxymethyl-lysine (CML) and pyrraline (Kuzan, 2021). Additional criteria encompass molecular weight (low vs. high), precursors (e.g., glucose-derived or lipid-derived), and toxicity, where toxic AGEs like glyceraldehyde-derived ones induce inflammation (Song et al., 2021). Protein glycation has primarily been associated with aging and various human diseases (Perrone et al., 2020; Rabbani and Thornalley, 2021). However, there is growing evidence that bacteria, despite their short lifespan, can also accumulate glycated products (Boteva and Mironova, 2019; Cohen-Or et al. 2011, 2013; Kram and Finkel, 2015; Mironova et al., 2001, 2005; Potts et al., 2005). Several studies have shown that AGE production can lead to proteotoxic effects and facilitate protein unfolding and aggregation (Iannuzzi et al., 2014). Despite that glycation often results in insoluble cross-linked products (Fournet et al., 2018; Iannuzzi et al., 2014; Rabbani and Thornalley, 2021), the aggregates detected in *E. coli* exposed to desiccation-rehydration stress contain a

relatively low level of AGEs, most glycation products remain soluble (Łupkowska et al., 2023).

Osmolytes in Bacterial Proteostasis and Protein Aggregation

Bacteria accumulate compatible solutes, or osmolytes, in response to environmental stresses such as high osmolarity, desiccation, and heat (Wood, 2015). These small, highly soluble organic molecules maintain cellular turgor while stabilizing native protein structures and suppressing non-specific aggregation (Khan et al., 2023). The primary mechanism is preferential exclusion: osmolytes are excluded from the protein's hydration layer, creating a thermodynamically unfavorable situation for the unfolded state by increasing free energy upon exposure of larger surface areas (Pepelnjak et al., 2024). This shifts the equilibrium toward the compact native state, reducing aggregation-prone intermediates and acting as chemical chaperones (Miotto et al., 2024). While preferential exclusion is universal, osmolytes vary in molecular implementation and efficacy, enabling bacteria to tailor responses to specific challenges (Burg and Ferraris, 2008; Mukherjee and Mondal, 2018). Building on these fundamental biophysical principles, osmolytes function in the crowded intracellular environment as precise modulators of the proteome, with effects dynamically calibrated by regulatory networks (Pepelnjak et al., 2024; Wood, 2015). Osmolyte accumulation is a programmed response to stress signals; cells control transport of osmolytes (Perroud and Le Rudulier, 1985) and their synthesis (Ruhal et al., 2013). By integrating osmolyte action into inducible defense pathways, bacteria proactively remodel their intracellular environment to counteract misfolding and aggregation while dynamically adjusting proteome solubility and assembly states (Brauer et al. 2023). While osmolytes are renowned for suppressing non-functional aggregation, emerging evidence shows that under specific conditions, these solutes can promote structured, functional protein aggregates (Kushwah et al., 2020). This dual functionality highlights sophisticated cellular control, where osmolytes serve as protective agents and key effectors in proteome organization. Their influence is context-dependent, varying by osmolyte, concentration, and protein involved (Patel et al., 2017).

Betaine Modes of Action

Betaine (glycine betaine), a potent zwitterionic methylamine, suppresses protein aggregation through strong preferential exclusion (Singh et al., 2009). It interacts unfavorably with the peptide backbone and side chains, raising the chemical potential of the unfolded state more than the native one, thereby favoring compact conformations and preventing unfolding that precedes aggregation (Shek and Chalikian, 2013). This passive stabilization positions betaine as an effective chemical chaperone (Leibly et al., 2012). Bacteria typically do not synthesize betaine *de novo* and betaine's preferential exclusion is deployed as part of a sophisticated regulatory strategy. It has a tightly regulated uptake via high-affinity systems (ProU/ProP), activated by the EnvZ/OmpR two-component system in response to osmotic stress (Jung et al., 2001; May et al., 1986). This regulated accumulation enables context-dependent effects (Morbach and Krämer, 2004). At physiological concentrations, betaine optimizes cytoplasmic solvent properties to favor native protein states (Cayley and Record, 2003). However, cells avoid over-accumulation, as excessive levels can over-stabilize proteins and inhibit functional dynamics (Cayley and Record, 2003). Betaine exhibits client specificity, effectively countering amorphous aggregation from osmotic stress but less so for amyloid fibrils (Li et al., 2013). It also synergizes with ATP-dependent chaperones like DnaK/J and GroEL/ES by reducing misfolded protein burden (Ravitchandirane et al., 2022). Ultimately, regulated betaine uptake allows the cell to fine-tune its cytoplasmic solvent, acting as a regulated solvent tuner that makes aggregation less favorable for the bulk proteome (Sleator and Hill, 2002). Emerging evidence indicates that betaine’s influence is context-dependent rather than monolithic. Under specific conditions, it can promote functional protein structures, demonstrating sophisticated dualism (Natalello et al., 2009). Betaine, by favoring compact states, stabilizes native, often oligomeric, protein forms (Borzova et al., 2022). While protective, this effectively "induces" assembly from monomers; for proteins functioning as large complexes, it shifts equilibrium toward the assembled form. Betaine's dual role is evident in its interaction with bacterial curli fibers, a functional amyloid system (Sleutel et al., 2017). Research shows betaine enhances *in vitro* assembly of the major curli subunit Curli specific gene A (CsgA) into amyloid fibrils (Sleutel et al., 2017). Preferential exclusion from the beta-

sheet surface of growing fibrils thermodynamically accelerates nucleation and elongation. Here, betaine catalyzes formation of structured, functional aggregates essential for biofilm formation and adhesion (Sleutel et al., 2017).

Carnosine Modes of Action

Carnosine (β-alanyl-L-histidine), a dipeptide, employs diverse active mechanisms to counter protein aggregation (Caruso et al., 2023). The histidine imidazole ring chelates transition metals (e.g., Cu^{2+}, Fe^{2+}), preventing Reactive Oxygen Species (ROS) formation via Fenton chemistry and subsequent oxidative protein damage (Boldyrev et al., 2013). It quenches reactive carbonyls (e.g., malondialdehyde) from lipid peroxidation, averting protein cross-linking (Jukić et al., 2021). Carnosine interacts with aggregation-prone peptides, destabilizing oligomers or fibrils (Caruso, 2022). Though exhibiting weak preferential exclusion, carnosine's primary actions target chemical triggers of protein damage rather than solvent thermodynamics (Caruso, 2022). Carnosine's mechanistic diversity enables it to function as a specialized, context-dependent modulator when available (Boldyrev et al., 2013). Though not a primary endogenous osmolyte in most prokaryotes, its uptake—likely via peptide transport systems in response to environmental availability—renders it a facultative component of the stress repertoire, fine-tuning proteome responses to specific insults (Caruso, 2022). Carnosine's modulatory role is pronounced under oxidative and metabolic stress, where it targets aggregation triggers, providing protection distinct from canonical chaperones and integrating with genetically regulated oxidative stress pathways like the *OxyR* regulon as a complementary non-enzymatic buffer (Kram and Finkel, 2014). Paradoxically, carnosine's interactive nature can influence aggregation pathways, sometimes steering toward structured, potentially functional amyloid forms. Under specific conditions, carnosine accelerates amyloid fibril formation from proteins like α-synuclein and Amyloid beta (Aβ) peptide (Wu et al., 2013). It binds early oligomeric species or nucleation sites, destabilizing off-pathway aggregates and promoting reorganization into ordered cross-β-sheet structures of mature fibrils (Wu et al., 2013). This acceleration often reduces aggregate cytotoxicity by promoting large, inert fibrils over small, toxic oligomeric intermediates (Kim and Seidler, 2011).

Trehalose Modes of Action

Trehalose, a non-reducing glucose disaccharide, uses a dual mechanism to prevent protein aggregation across stress conditions: Water Replacement Hypothesis, where during desiccation or extreme osmotic stress, trehalose forms an amorphous glassy state, hydrogen-bonding with protein polar groups to replace hydration shell water and avert dehydration-induced unfolding (Khalifeh et al., 2019); and Preferential Exclusion (Chemical Chaperoning), where in aqueous solutions, trehalose's strong exclusion from protein surfaces thermodynamically stabilizes the native fold by elevating the unfolded state's free energy (Kaushik et al., 2003). These context-dependent mechanisms—direct interaction in dehydrated states and indirect exclusion in hydrated ones—enhance trehalose's efficacy in maintaining protein solubility and structure. Trehalose's mechanistic versatility is harnessed through a tightly regulated biosynthetic program, elevating it from a passive stabilizer to a master stress integrator (Vanaporn and Titball, 2020). Its production is controlled at transcriptional and metabolic levels, with the *otsAB* operon regulated by the general stress sigma factor RpoS and linked to central carbon metabolism (Strom and Kaasen, 1993). Nevertheless, trehalose's properties that enable stabilization—crowding the molecular environment and altering water activity—can drive assembly of specific functional protein structures. In *E. coli*, high intracellular trehalose concentrations can modulate amyloid-like aggregate assembly, influencing liquid-liquid phase separation (LLPS), a process forming membraneless organelles (Kuczyńska-Wiśnik et al., 2023). While often suppressing LLPS by stabilizing folded proteins, its effect is concentration- and system-dependent (Łupkowska et al., 2023). By altering solvent quality and interactions, trehalose modulates condensate properties, potentially driving maturation or assembly within them. This fine-tunes cytoplasmic spatial organization.

II. Aims

Previous studies have demonstrated that during desiccation/rehydration stress, *E. coli* accumulates protein aggregates and glycation products, both of which are primarily considered to exert toxic effects on the cell. Comparable levels of protein aggregates were detected in viable and dead cells, whereas glycation products were mainly localized in dead cells (Łupkowska et al., 2023). These results suggested that glycation, rather than protein aggregation, was the leading cause of cell death under desiccation stress.

This thesis aims to verify this hypothesis and extend the study of stress-induced protein aggregation and glycation in two Enterobacteriaceae: *E. coli* and *K. pneumoniae*. The following experiments were planned:

1. Analysis of the effects of selected osmolytes (betaine, carnosine, and trehalose) on protein glycation, aggregation, and cell viability in *E. coli* and the *K. pneumoniae* reference strain MKP103, when exposed to desiccation and rehydration stress.
2. Investigation of the effect of lysine acetylation on *E. coli* protein glycation *in vivo* and *in vitro.* Since both glycation and acetylation may occur on the lysine residue, it seems that these two types of modification compete with each other. Different studies demonstrated that acetylation postpones or inhibits glycation (Nahomi et al., 2013; Zheng et al., 2019).
3. Investigation of the relationship between cell viability, protein aggregation, and glycation in macrocolonies of the *K. pneumoniae* clinical isolate BA-577. These macrocolonies are composed of a mucoid center and a non-mucoid ring. It is hypothesized that the ring subpopulation, which lacks a capsule, is more exposed to desiccation compared to the center of the macrocolonies.
4. To reveal the mechanisms underlying these differences, including the presence or absence of a capsule, and to better characterize the subpopulations, analyses using NGS data have been conducted.

III. Materials and Methods

III.1 Bacterial strains

Table 2. Bacterial strains used during research

Name	Produced by
E. coli (MC4100), F^- *araD139* Δ(*argF-lac*)U169 *rpsL150 relA1 flbB5301 fruA25 deoC1 ptsF25*	Department of General and Medical Biochemistry collection
E. coli BW25113 [F−, Δ(*araD-araB*)567, *lacZ*4787(del):*rrnB*-3, λ−, rph-1, Δ(*rhaD-rhaB*), *hsdR*514]	Keio collection
E. coli BW25113 Δ*ackA-pta*	Department of General and Medical Biochemistry collection
E. coli BW25113 *ΔackA-pta-pka*	Department of General and Medical Biochemistry collection
K. pneumoniae 577-BA (clinical isolate)	Collection of Plasmids and Microorganisms, Faculty of Biology
K. pneumoniae MKP103, a derivative of KPNIH1, lacking the carbapenemase gene	Manoil lab, USA. https://www.gs.washington.edu/labs/manoil/kpneumoniae_library.htm

KPNIH1 was first identified during a hospital outbreak at the U.S. National Institutes of Health (NIH) Clinical Center and is also known as KPNIH1 (Conlan et al., 2014, 2016; Snitkin et al., 2012).

III.2 Culture Growth and Stress Treatment

Table 3. Medium for bacterial growth

Acronym/Name		Amount / Concentration	Supplier and Product number
Lysogeny Broth (1 L)	NaCl	10 g	Avantor Performance Materials Poland S.A. (Cat. No. BA4121116), Gliwice, Poland
	Yeast Extract	5 g	Servabacter®, SERVA Electrophoresis GmbH, Heidelberg, Germany (24540.02) 500 g

	Tryptone	10 g	BioMaxima S.A., Lublin, Poland (PB 02)
LB-agar plates (1 L)	Agar	15 g	Bacteriological Lab-Agar™, BioMaxima S.A., Lublin, Poland (AB 03- 500)

E. coli: The *E. coli* strain MC4100 was cultivated at 37 ℃ in 100 mL of Lysogeny Broth (LB) medium within Erlenmeyer flasks under agitation. Upon reaching an OD_{595} of 0.5, the cells were centrifuged, resuspended in 5 mL of spent medium (achieving a 20-fold concentration relative to the original culture), and subjected to desiccation in an open Petri dish at 21 ℃ and approximately 40% relative humidity. Following complete desiccation (approximately 4 h), the bacteria were rehydrated in 10 mL of 0.9% NaCl (resulting in a 10-fold concentration compared to the original culture), divided into two 5 mL aliquots, and pelleted by centrifugation. One pellet served as the sample containing desiccated cells for subsequent experiments, while the other was resuspended in 10 mL of fresh LB medium and incubated for 40 min at 37 ℃ with agitation (rehydration stage).

***K. pneumoniae* MKP103:** An overnight culture of *K. pneumoniae* MKP103 was diluted 100-fold into 100 mL of the LB medium and grown with agitation until the OD_{595} reached 0.5. The entire 100 mL culture was then harvested by centrifugation at 330 × g for 15 min at 4 ℃. After discarding the supernatant, the cell pellet was resuspended in 5 mL of 0.9% (weight per volume, w/v) NaCl solution (saline), resulting in a 20-fold concentration of the original culture. This cell suspension was transferred to a Petri dish and desiccated in an incubator at 37 ℃ for three days and two days into complete desiccation (aka storage time).

Following desiccation, the dried cells were resuspended in 10 mL of saline, creating a suspension 10-fold more concentrated than the original culture. This suspension was immediately divided into two 5 mL aliquots, designated A (Desiccated) and B (Rehydrated).

***K. pneumoniae* 577-BA:** To generate the *K. pneumoniae* macrocolonies, five 10-µL droplets of strain 577 overnight culture were spotted onto 5–6 agar plates and

incubated at 37 ℃ for five days to ensure the full development of the desired regions (the center and ring).

1. **Sample processing for protein aggregates extraction (*E. coli*, *K. pneumoniae* MKP103)**

   - **Desiccated Sample (Aliquot A):** From the 5 mL desiccated aliquot, a 1 mL sample was collected to serve as the "total desiccated protein extract." The remaining 4 mL was designated for desiccated aggregate extraction. Both samples were centrifuged, washed with saline, centrifuged again, and the resulting pellets were stored at -20 ℃.
   - **Rehydrated Sample (Aliquot B):** The 5 mL rehydrated aliquot was centrifuged as described above. The pellet was then resuspended in 10 mL of LB and incubated at 37 ℃ for 40 min to permit recovery. Following this rehydration period, a 1 mL sample was collected ("total rehydrated protein extract") and the remaining 4 mL was designated for rehydrated aggregate extraction. Both samples were processed as described for Aliquot A.

III.3 Determination of the number of culturable, VBNC and dead cells

Cell viability was determined using the LIVE/DEAD™ *Bac*Light™ Bacterial Viability Kit, containing SYTO® 9 and propidium iodide (PI). Bacterial cells from 5 mL of culture were pelleted by centrifugation (330 × g, 15 min, 4 ℃), resuspended in 1 mL of 0.9% (w/v) saline, and diluted as needed (1:10 or 1:100) to an appropriate density for microscopy. A 100 $\mu\mathrm{L}$ volume of the cell suspension was then incubated with 0.3 $\mu\mathrm{L}$ of the stain mixture for 6–7 minutes in the dark. Finally, 5 $\mu\mathrm{L}$ of the stained sample was pipetted onto a Neubauer counting chamber, and live (green) and dead (red) cells were counted within the 25 central squares of the hemacytometer grid under a fluorescence microscope to calculate viability. colony-forming units (CFU) counts (culturable bacteria) were estimated by plating serial dilutions on LB agar plates. The number of viable-but-non-culturable (VBNC) cells was calculated by subtracting CFU counts from the number of PI-excluding cells.

Table 4. Live and Dead cell staining

Acronym/Name	Supplier and Product number
Live/Dead™ *Bac*Light™ Bacterial Viability Kits (1.67 $\mathbf{mM}$ SYTO™ 9 nucleic acid stain, 1.67 $\mathbf{mM}$ propidium iodide)	Invitrogen, Thermo Fisher Scientific, Oregon, USA (L7007)

III.4 Protein Aggregates extraction

Protein aggregates were isolated from *E. coli* as described previously (Kuczyńska-Wiśnik et al., 2016). Briefly:

1. **Initial Lysis and sonication:** Pelleted cells were converted into spheroplasts in the presence of lysozyme and were lysed by sonication.
2. **Wash:** Intact cells were then removed by centrifugation (2 000 × g, 15 min). The supernatant was incubated with 2% Triton X-100 for 15 min at room temperature. Insoluble protein aggregates were pelleted at 21 000 × g for 30 min and stored at $-20\ ℃$ for subsequent analysis.

The aggregate extraction protocol for *K. pneumoniae* was performed on the 4 mL samples from both the desiccated and rehydrated sets (III.2). The same procedure was used to isolate aggregates from the subpopulations of 577-BA macrocolonies.

1. **Initial Lysis:** The cell pellet was resuspended in a calculated volume of CelLytic™ B lysis reagent, prepared according to the manufacturer's protocol (**Table 5**). The solution was incubated for 20 min at room temperature ($\sim 22\ ℃$) with shaking.
2. **Sonication:** The lysate was then sonicated on ice for 10 cycles (1 minute on, 1 minute off cooling intervals) to ensure complete cell disruption.
3. **First Wash:** The sonicated solution was centrifuged (330 × g, 15 min), the supernatant was discarded, and the pellet was resuspended in the same volume of lysis reagent prepared without Benzonase®. This suspension was incubated for 20 min at room temperature with shaking.
4. **Second Wash:** Following centrifugation, the pellet was washed with a 1:100 dilution of the original CelLytic™ B reagent and centrifuged at 330 × g for 10 min.

5. **Storage:** After the final supernatant was discarded, the insoluble pellet, containing the protein aggregates, was resuspended in 100 μL of LB and stored at -20 ℃ for subsequent analysis.

Table 5. Aggregate extraction buffer

Name	Supplier and Product number
Benzonase® Nuclease (250 unit/$\mathbf{mL}$)	SIGMA-ALDRICH, Denmark (1003339500)
CelLytic™ B Cell Lysis Reagent	SIGMA-ALDRICH, USA (1003049801)
cOmplete™ Mini EDTA-free (protease inhibitor) in 5 $\mathbf{mL}$ $\mathbf{NaHPO_4}$	Roch Diagnostics GmbH, Mannheim, Germany (11836170001)
EDTA (0.5 M)	Disodium Salt: Dihydrate, SIGMA-ALDRICH CHEMIE GmbH, Steinheim, Germany (E-5513)
H_2O	
Lysozyme 100× (20 $\mathbf{mg/mL}$)	SERVA Electrophoresis GmbH, Heidelberg, Germany (Cat. No. 28263.02)

III.5 Isolation of the outer membrane (OM) and urea-SDS-PAGE

E. coli cells were resuspended in 0.2 M Tris-HCl buffer (pH 8.0) containing 20 mM sucrose, 0.2 mM EDTA and lysozyme (200 µg/ml) and incubated for 10 min at room temperature. The same volume of extraction buffer was added 2% Triton X-100, 50 mM Tris-HCl, 10 mM $MgCl_2$, Benzonase and the solution was incubated on ice for 30 min. The lysate was centrifuged at 2 500 × g for 5 min. The OM was isolated from the supernatant by centrifugation at 22 000 × g for 15 min. The pellet containing the OM was washed with Phosphate-based saline (PBS). The OM proteins were then separated using 8 M urea-8 % SDS-PAGE (Sodium dodecyl sulfate polyacrylamide gel electrophoresis).

Table 6. Outer membrane (OM) isolation buffer

Acronym/Name	Amount / Concentration	Supplier and Product number
Benzonase® Nuclease	10 $unit/mL$	SIGMA-ALDRICH, Denmark (1003339500)
EDTA	0.2 mM	Disodium Salt: Dihydrate, SIGMA-ALDRICH CHEMIE GmbH, Steinheim, Germany (E-5513)
Lysozyme	200 $\mu g/mL$	SERVA Electrophoresis GmbH, Heidelberg, Germany (Cat. No. 28263.02)

$\mathbf{MgCl_2.(6H_2O)}$	10 mM	Merck KGaA, Darmstadt, Germany (1374248-1G)
PBS	tablets	SIGMA-ALDRICH CHEMIE GmbH, Steinheim, Germany (79382-50TAB)
D(+)-Saccharose	20 mM	Carl Roth GmbH + Co KG, Karlsruhe, Germany (4661.2)
Triton™ X-100	2%	SIGMA-ALDRICH, MO, USA (93443-500ML)
Trizma® base	50 mM	SIGMA-ALDRICH CHEMIE GmbH, Steinheim, Germany (T6066-5KG)
Urea	8 M	ZOOM®, Invitrogen™, CA, USA (Cat. No. ZU10001)

III.6 Detection of *K. pneumoniae* capsule by Percoll density gradient centrifugation

The center and ring subpopulations of *K. pneumoniae* 577-BA were suspended in 0.5 mL of PBS to an OD_{595} of 0.3 and then layered on top of a two-step Percoll gradient (1 mL of 100% and 0.5 mL of 60% Percoll in PBS). The samples were centrifuged at 5000 rpm for 5 min at room temperature in the Eppendorf Mini Spin centrifuge.

Table 7. Percoll gradient

Acronym/Name	Amount / Concentration	Supplier and Product number
Percoll	100% (60% in PBS)	BioChemika, SIGMA-ALDRICH CHEMIE GmbH, Steinheim, Germany (77237-500ML)
PBS	Tablets	SIGMA-ALDRICH CHEMIE GmbH, Steinheim, Germany (79382-50TAB)

III.7 Fluorescent Advanced Glycation End (AGE) products measurement

Bacterial pellet of interest was proceeded for mere cell lysis according to the first two phases of III.4. Bacterial lysates were then excited at specific frequency by fluorospectrometer for detection of the emission spectra that would indicate the presence of the following AGE products: pentosidine-like (Ex: 335 nm/Em: 385 nm), vesperlysine C-like (Ex: 345 nm/Em: 404 nm), vesperlysine A/B-like (Ex: 366 nm/Em:

442 nm), lysyl-pyrropiridine-like (Ex: 370 nm/Em: 448 nm), FFI-like (Ex: 380 nm/Em: 440 nm) and fluorolink-like (Ex: 380 nm/Em: 460 nm).

III.8 Polyacrylamide Gel Electrophoresis (PAGE)

1. **Gel Preparation:** A discontinuous polyacrylamide (PAA) gel was prepared, consisting of a 12% resolving (running) gel and a 5% stacking gel (see **Table 8**–**Table 9** for compositions).

Table 8. Denaturing 12% gel for SDS-PAGE for the Running Gel

Acronym/Name	Amount / Concentration	Supplier and Product number
Acrylamide N,N'-Methylene-bis-Acrylamide	30%	SIGMA-ALDRICH CHEMIE GmbH, Steinheim, Germany (A3553-1KG, M-7279)
APS (Ammonium persulfate)	10%	SIGMA-ALDRICH CHEMIE GmbH, Steinheim, Germany (A3678-25G)
H_2O	5 mL	
SDS	10%	BioShop® Canada Inc., ON, Canada (SDS001.1)
TEMED (tetramethylethylenediamine)	15 µL	SIGMA-ALDRICH CHEMIE GmbH, Steinheim, Germany (T-9281)
Tris (pH 8.8)	1.5 M	SIGMA-ALDRICH CHEMIE GmbH, Steinheim, Germany (T6066-5KG)

Table 9. Denaturing 5.1% gel for SDS-PAGE for the Stacking Gel.

Acronym/Name	Amount / Concentration	Supplier and Product number
Acrylamide	0.66 mL 24%	SIGMA-ALDRICH CHEMIE GmbH, Steinheim, Germany (A3553-1KG)
APS	40 µL 10%	SIGMA-ALDRICH CHEMIE GmbH, Steinheim, Germany (A3678-25G)
H_2O	2.74 mL	
SDS	40 µL 10%	BioShop® Canada Inc., ON, Canada (SDS001.1)
TEMED	8 µL	SIGMA-ALDRICH CHEMIE GmbH, Steinheim, Germany (T-9281)

Tris (pH 6.8)	0.5 mL 1M	SIGMA-ALDRICH CHEMIE GmbH, Steinheim, Germany (T6066-5KG)

2. **Sample Preparation:** Protein samples were normalized to a target concentration of 100 ng/µL. The samples were then mixed with loading buffer (**Table 10**) at a 2:1 ratio (volume of solute per volume of mixture [v/v], protein to buffer). These mixtures were transferred to 1.5 mL tubes, denatured by heating at 99 ℃ for 5 min in a heat block, and then immediately cooled on ice.

Table 10. 2× Loading buffer and Ladder

Acronym/Name	Amount / Concentration	Supplier and Product number
Bromophenol blue sodium salt, for electrophoresis	0.0012%	SIGMA-ALDRICH CHEMIE GmbH, Steinheim, Germany (B5525-25G)
DTT (Dithiothreitol)	100 mM	SERVA Electrophoresis GmbH, Heidelberg, Germany (Cat. No. 20710.04)
Glycerol	10%	Serva Electrophoresis GmbH, Heidelberg, Germany (Cat. No. 23176.01)
SDS Electrophoresis Grade	2%	BioShop® Canada Inc., ON, Canada (SDS001.1)
Trizma® base	62.5 mM	SIGMA-ALDRICH CHEMIE GmbH, Steinheim, Germany (T6066-5KG)
Ladder, 3-color Prestained, Protein Marker (10–245 kDa)	2.5 µL	BLIRT S.A., Gdańsk, Poland (PM30-500)

3. **Electrophoresis:** The polymerized gel, secured in its casting plates, was placed in a vertical electrophoresis unit. The inner and outer chambers of the unit were filled with 1× running buffer (**Table 11**). The prepared samples and a molecular weight marker were loaded into the wells. Electrophoresis was conducted at a constant current of 50 V until the dye front exited the stacking gel, at which point the current was increased to 100 V for the remainder of the separation through the resolving gel. To probe the total transfer of proteins from the PAA gel, a replicate gel was stained with

Coomassie for 10 min and was destained in several washes by the same mixture (**Table 12**) without the blue pigment to visualize possible protein contents remaining in the gel.

Table 11. 5× Migration buffer

Acronym/Name	Amount / Concentration	Supplier and Product number
Glycine	190 mM	EUROCHEM BGD, Tarnów, Poland
SDS	0.1%	BioShop® Canada Inc., ON, Canada (SDS001.1)
Trizma™ base	25 mM	SIGMA-ALDRICH CHEMIE GmbH, Steinheim, Germany (T6066-5KG)

Table 12. Reagents for Coomassie Briliant Blue stain

Acronym/Name	Amount / Concentration	Supplier and Product number
Acetic acid	50%	Avantor, Gliwice, Poland (BA8760114.1000)
Coomassie® Brilliant Blue R	0.25%	SIGMA-ALDRICH, Merck KGaA, Darmstadt, Germany (27816)
Methanol	10%	Avantor, Gliwice, Poland (Cat. No. BA 1990110)

III.9 Protein Immunodetection (Western immunoblotting)

Proteins were transferred from a gel to a nitrocellulose membrane in electrotransfer buffer at a sum of 1,000 mA for 1 h at room temperature. After the electrotransfer, the membrane was stained with 0.1% Ponceau solution for 10 min on a rocker to confirm protein transfer. The membrane was then rinsed with TBST to remove the stain.

Table 13. Electrotransfer buffer

Acronym/Name	Amount / Concentration	Supplier and Product number
Glycine	190 mM	EUROCHEM BGD, Tarnów, Poland
Methanol	10%	Avantor, Gliwice, Poland (Cat. No. BA 1990110)

Nitrocellulose blotting membrane	6 × 7 cm	Amersham™ Protran™ 0.2 µM NC, Karlsruhe, Germany (Cat. No. 10600001)
Trizma™ base	25 mM	SIGMA-ALDRICH CHEMIE GmbH, Steinheim, Germany (T6066-5KG)

1. The membrane wasembrane was then incubated in a solution of primary antibodies for 1 h at room temperature and washed three times in TBST (0.05% Tween 20) for 10 min each, followed by 1 h incubation with secondary antibodies and final wash in TBST. SuperSignal™ West Pico PLUS Chemiluminescent kit was used to detect antigen-antibody complexes. The membrane was visualized in a C400 Azure visible fluorescent imager.

Major products of protein oxidation (i.e., carbonyl groups) were detected upon derivatizing of protein extracts with dinitrophenylhydrazine (DNPH) as described previously (Matuszewska et al., 2008).

Table 14. Ponceau S dye solution

Acronym/Name	Supplier and Product number
0.1% Acetic acid	Avantor, Gliwice, Poland (BA8760114.1000)
0.5% Ponceau S	Merck KGaA, Darmstadt, Germany (P-3504)

Table 15. Tris-buffered Saline + Tween (TBST)

Acronym/Name		Amount / Concentration	Supplier and Product number
TBS	KCl	27 mM	SIGMA-ALDRICH CHEMIE GmbH, Steinheim, Germany (T6066-5KG; P-4504-1KG)
	NaCl	150 mM	
	Trizma™	15 mM	
Tween 20		0.1%	BioShop® Canada Inc., ON, Canada (TWN508.500)

Table 16. Immunodetection (Western blotting)

Acronym/Name		Supplier and Product number
Primary antibodies	Mouse Monoclonal Elongation factor thermo unstable (EF-Tu) antibody	Hycult Biotech Inc., PA, USA (HM6010)

	Rabbit Polyclonal Acetyl Lysine (AcK) Antibody	Merck KGaA, Darmstadt, Germany (AB3879)
	Rabbit Polyclonal Carboxymethyl-Lysine (CML) Antibody	Abcam Limited, MA, USA (Ab27684)
	Rabbit Polyclonal dinitrophenyl (DNP) antibodies	Merck KGaA, Darmstadt, Germany (D9656)
Secondary antibodies	Goat Anti-Rabbit IgG H&L (HRP)	Abcam Limited, MA, USA (Ab6721)
Luminol/Enhancer (kit 34580)		SuperSignal™ West Pico PLUS Chemiluminescent Substrate, Thermo Scientific, IL, USA (Lot# WF326283)
Stable Peroxide (kit 34580)		

Table 17. Primary and secondary antibodies

Primary antibody & concentration		Secondary antibody & concentration	
Anti-AcK	1:1000	Anti-Rabbit IgG	1:3000
Anti-CML	1:1000		
Anti-DNP	1:1000		
EF-Tu	1:500	Anti-Mouse IgG	1:5000

III.10 Lipid peroxidation assay

The thiobarbituric acid-reactive substances (TBARS) assay was performed to detect malondialdehyde, the end product of lipid peroxidation and an indirect indicative of ROS production. The reaction mixture was prepared according to the Lipid Peroxidation Assay kit. The MDA-TBA adducts were quantified colorimetrically at 532 nm.

Table 18. Lipid Peroxidation (malondialdehyde [MDA]) Assay Kit

Acronym/Name	Supplier and Product number
BHT, 100×	Merck KGaA, Darmstadt, Germany (Cat. No. MAK085)
MDA Lysis Buffer	
MDA Standard, 4.17 M	
Phosphotungstic Acid Solution	

TBA	

III.11 Genome Sequencing and Bioinformatic Analysis

Genomic DNA isolated from both the ring and the center was sequenced by Genomed S.A. (Poland). DNA was fragmented by sonication with a Covaris E210 using parameters recommended for Illumina library preparation. Libraries were prepared with the NEBNext Ultra II DNA Library Prep Kit for Illumina according to the manufacturer's instructions. Sequencing was performed on an Aviti device in paired-end mode with read lengths of 2x300 nt. Sequence quality control was performed with Fastp version 0.23.4. Genome assembly was performed with metaviralSPAdes version 3.15.5. Genome comparison was performed using Mauve.

1. **Circular genome maps**: The Fast-All (fast A; FASTA) data were then analyzed, using Proksee v1.8.2, annotated with Bakta tool. Circular genome maps per both center and ring subpopulations were created to show overall structure, GC skew, and gene density to provide a high-level view before diving into differences (**Figure 23**).

2. **Sequence Alignment of subpopulations:** *De novo* genome assemblies were generated for the Ring and Center subpopulations of *K. pneumoniae* strain 577-BA using short-read NGS data in Proksee v1.8.2, annotated with Bakta tool. Assemblies were produced in both contig and scaffold formats, with low-coverage and short contigs (<500 bp) filtered out to enhance quality. Key metrics for these assemblies are summarized in V.3.

   In order to measure the mean nucleotide identity between the *K. pneumoniae* 577-BA ring and center subpopulations, “center” and “ring” subpopulations genomes were used as “reference” (A) and “query” (B), respectively. Orthologous matches were clarified, using Galaxy.eu, annotated with Fast Average Nucleotide Identity (ANI; FastANI) tool.

IV. Results

IV.1 Influence of osmolytes on *E. coli* cell viability, the formation of protein aggregates and glycation products

Previous studies have demonstrated that carnosine can inhibit the accumulation of CML in aging *E. coli* MC4100 cultures and protect *E. coli* against MGO toxicity (Pepper et al., 2010). Therefore, carnosine was expected to improve *E. coli* survival and inhibit protein aggregation and glycation under desiccation-rehydration stress.

IV.1.1 Carnosine enhances viability of the *E. coli* exposed to desiccation-rehydration stress

During 4 hours of desiccation, the control *E. coli* MC4100 cultures displayed low culturability (~10–15%), high dead cell proportions (> ~30%), and comparable VBNC cells (~30%), as assessed using the LIVE/DEAD *Bac*Light viability kit according to the III.3. This profile highlights the profound impacts of desiccation stress, including water deprivation-induced osmotic imbalances, oxidative damage, and membrane disruption, which collectively suppress metabolic activity and propel a significant subset of cells into the VBNC state—a dormant, resilient phenotype that maintains viability without culturability on standard media. In the presence of 0.45% carnosine, culturability remained similar (~15%), but dead cells decreased substantially (~20%), and VBNC cells escalated to ~60% with high statistical significance (***, $P < 0.001$). These alterations indicate carnosine's protective capacity, likely through its antiglycative and antioxidant properties that scavenge reactive carbonyl species, stabilize proteins against misfolding (Caruso, 2022), and facilitate adaptive dormancy, thereby enhancing overall desiccation tolerance compared to controls.

Following 40 minutes of rehydration in LB, control cultures exhibited a slight rise in culturable cells (~20%) over desiccated levels, sustained high dead cell fractions but no tangible fluctuation, a decline in VBNC cells (< ~20%). This suggests incomplete recovery, where abrupt water influx during rehydration exacerbates cellular damage in stressed populations, potentially via osmotic shock or unresolved oxidative burdens, limiting VBNC resuscitation and promoting lysis. Conversely, 0.45% carnosine treatment

yielded a significant boost in culturable cells (> ~40%; **, P < 0.01), a modest non-significant reduction in dead cells (~30%), persistently elevated VBNC cells (~30%; *, P < 0.05). This enhanced resuscitation efficiency underscores carnosine's role in mitigating rehydration stress, possibly by preserving membrane integrity and enabling the revival of VBNC populations through sustained osmoprotection and attenuation of glycation during the recovery phase.

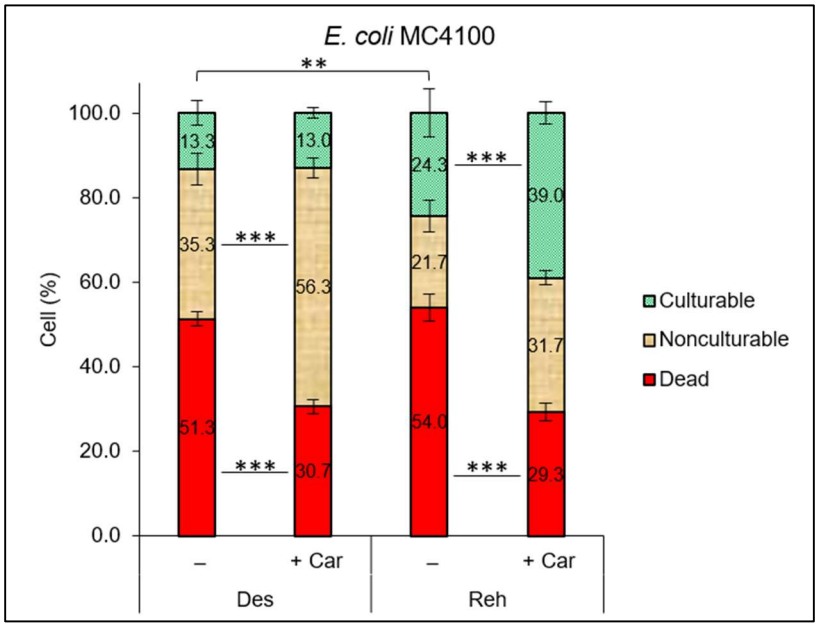

Figure 1. The influence of carnosine on *E. coli* culturability and viability under desiccation-rehydration stress. *E. coli* cultures were grown in LB, without and with 0.45% carnosine to an OD_{595} of 0.5. then exposed to 4 h of desiccation (Des.), followed by 40 min of rehydration (Reh.). The percentages of culturable, viable-but-non-culturable (VBNC), and dead cells in *E. coli* populations were estimated as described in section III.3. Error bars represent the standard deviation of three values. Statistical significance was determined by two-way ANOVA with Tukey's test for multiple comparisons (*P < 0.05; **P < 0.01; ***P < 0.001).

IV.1.2 Carnosine inhibits the formation of protein aggregates in *E. coli* exposed to desiccation/rehydration stress

Protein aggregates were isolated from *E. coli* MC4100 according to the III.4. To determine how 0.45% concentration of carnosine influences *E. coli* protein aggregate formation caused by desiccation-rehydration stress, the percentage of protein aggregates (compared to total protein) was measured via SDS-PAGE and densitometry at three different stages: before desiccation [control culture, log phase (OD_{595} = 0.5] after desiccation (4 h), and rehydration (40 min). Log-phase bacteria, grown with or

without carnosine, showed negligible aggregation, as expected in a healthy growing culture (**Figure 2**). Four hours of desiccation significantly increased protein aggregation (~0.5% of total protein) in bacteria growing without carnosine. During the subsequent rehydration stage, the level of protein aggregates reached ~2.5%. Carnosine significantly inhibited aggregation during desiccation (by ~60% compared to the culture without carnosine) and rehydration (~40%). These results suggested that trehalose may stabilize protein structures or prevent their misfolding.

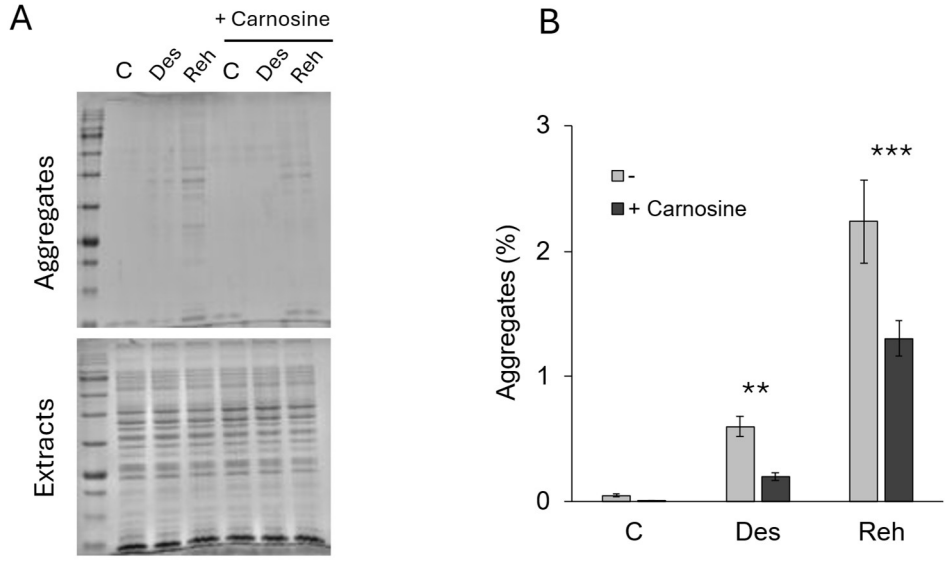

Figure 2. The influence of carnosine on the formation of protein aggregates in *E. coli* under desiccation-rehydration stress; **A)** Protein aggregates were isolated as described in III.5. The aggregates and whole cell extracts were resolved by SDS-PAGE and stained with Coomassie, then analyzed by densitometry using ImageJ software. Representative gels are shown; **B)** The graph in clustered columns format shows quantification of aggregate formation. Error bars represent the standard deviation of three values. Statistical significance was determined by two-way ANOVA with Tukey's test for multiple comparisons ($P < 0.05$, marked *; $P < 0.01$, marked **; $P < 0.001$, marked ***).

IV.1.3 The accumulation of AGE products in *E. coli* is diminished by carnosine

To determine the influence of carnosine on the formation of glycation products during desiccation-rehydration stress, fluorescent AGEs (**Figure 3**), and CML (**Figure 4**) were detected according to the excitation wavelengths as per III.8 were used to detect glycation products that exhibit maximum fluorescence at a specific emission wavelength upon excitation at 335, 345, 366, 370 and 380 nm (Séro et al., 2013). It was found that

carnosine significantly inhibited the formation of fluorescent AGEs (**Figure 3**). The relative levels of vesperlysine A/B and C-like products were decreased in the presence of carnosine even before desiccation. The medium in which *E. coli* was resuspended during rehydration was not supplemented with carnosine thus no major differences in fluorescence levels were observed after rehydration.

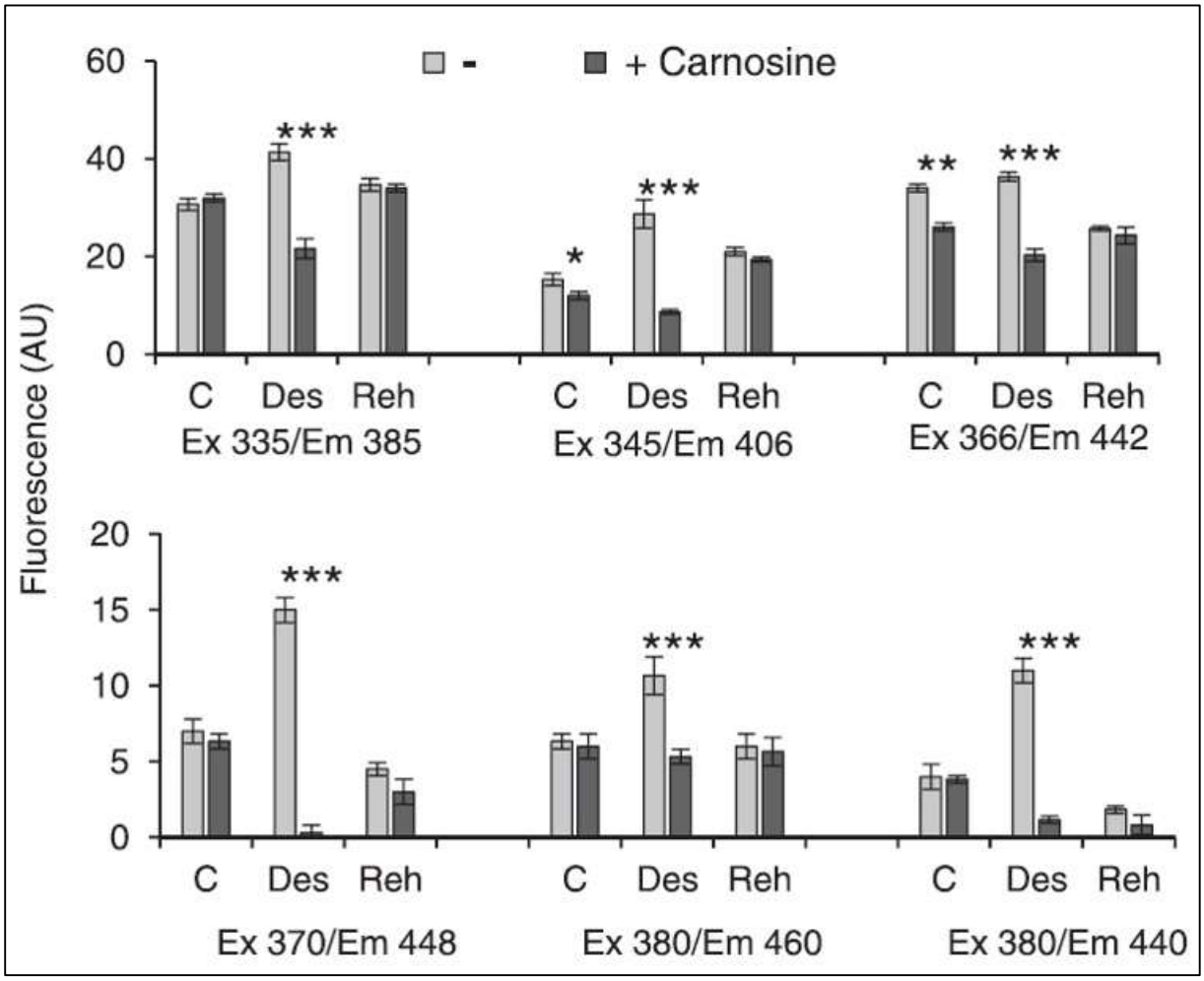

Figure 3. Influence of carnosine on the formation of fluorescent AGEs in *E. coli* cultures exposed to desiccation-rehydration stress. The graph depicts a quantification of fluorescence intensity in Arbitrary Units (a.u.) of various glycation products under three conditions: C- control culture (log phase) (at OD_{595} 0.5), Des (4 h desiccation), Reh (40 min rehydration) in *E. coli* cells. Six different fluorescence excitation/emission settings correspond to six types of glycation-like products; upper row: Ex 335 / Em 385 (Excitation [Ex.] at 335 nm and emission [Em.] at 385 nm) for pentosidine-like, Ex 345 / Em 406 for vesperlysine C-like, Ex 366 / Em 442 for vesperlysine A/B-like; and lower row: Ex 370 / Em 448 for lysyl-pyrropiridine-like, Ex 380/Em 460 for fluorolink-like, Ex 380 / Em 440 for FFI-like. Statistical significance was determined by two-way ANOVA with Tukey's test for multiple comparisons (*P < 0.05; **P < 0.01; ***P < 0.001).

Consistent with the above results, carnosine also inhibited CML formation (**Figure 4**). In the absence of carnosine, a modest increase (~1.2-fold) of CML level was observed after desiccation, suggesting initial glycation during drying due to concentrated carbonyl species and reduced metabolic turnover. After rehydration, a significant elevation (~1.8-fold) in CML levels was detected, indicating a burst of Maillard reactions upon water influx, possibly driven by reactive oxygen species (ROS) or by mobilized reducing sugars reacting with lysine residues. Carnosine did not alter basal CML levels in unstressed cells but reduced CML formation under stress, particularly after rehydration.

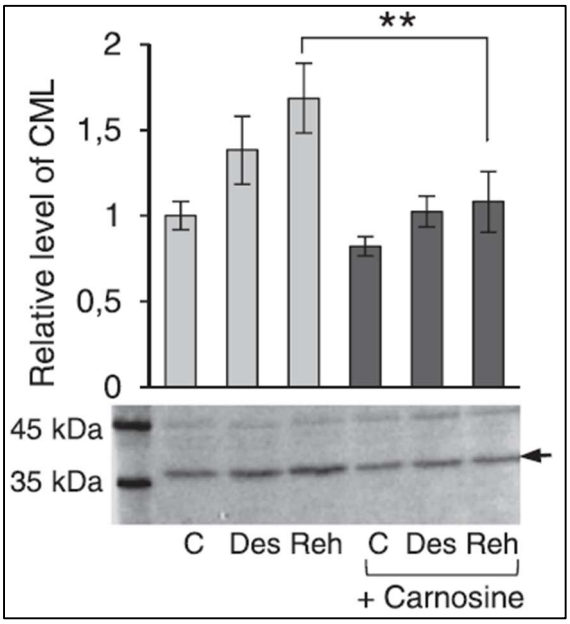

Figure 4. The influence of carnosine on CML accumulation in *E. coli* exposed to desiccation-rehydration stress. *E. coli* cultures were grown in LB, with or without 0.45% carnosine, to an OD_{595} of 0.5, then exposed to 4 h of desiccation, followed by 40 min of rehydration in LB. CML was detected (a.u.) via immunoblotting using anti-CML antibodies (C, control culture [log phase], Des. desiccation, Reh. rehydration). Statistical significance was determined by two-way ANOVA with Tukey's test for multiple comparisons (*P < 0.05; **P < 0.01; ***P < 0.001).

IV.1.4 Upon desiccation-rehydration stress, carnosine inhibits lipid peroxidation but not protein oxidation

The protective role of carnosine is often attributed to its antioxidant activity (Chmielewska et al., 2020; Jukić et al., 2021). Protein carbonyls formed during oxidation are irreversible modifications that promote unfolding, crosslinking, and aggregation,

rendering proteins protease-resistant and cytotoxic. This ties directly to glycation (e.g., CML in **Figure 4**), as oxidative stress and Maillard reactions are interconnected—ROS accelerate glycation, and AGEs sensitize proteins to oxidation (glycoxidation). On this basis, the effects of carnosine on protein oxidation were examined. A mild increase (~1.3-fold) in DNP-derivatives of carbonyl groups was observed after desiccation in the culture without carnosine, reflecting limited oxidative stress during drying, possibly due to residual metabolism or auto-oxidation in the concentrated state. Rehydration resulted in a pronounced spike (~1.7-fold, **), highlighting a rehydration-associated oxidative burst, likely driven by rapid ROS generation upon water influx and metabolic reactivation. Carnosine did not affect steady-state oxidation in unstressed cells, exerted minimal antioxidant protection during the desiccation phase, and demonstrated no suppression of carbonyl formation during rehydration.

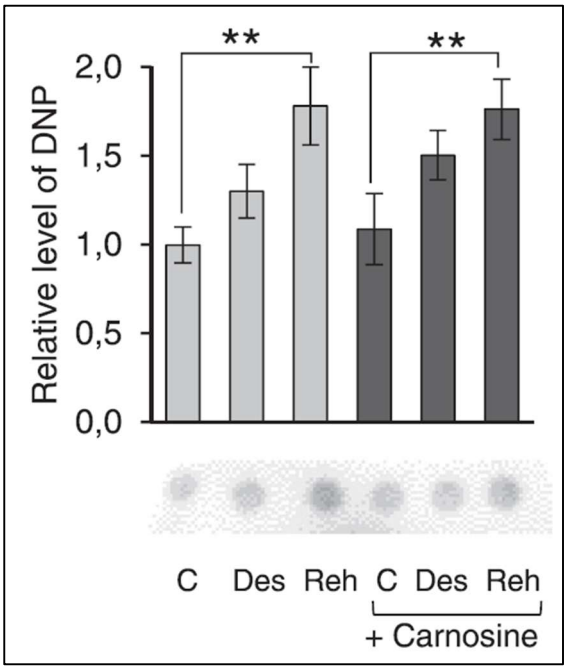

Figure 5. The influence of carnosine on the formation of carbonyl groups in *E. coli* exposed to desiccation-rehydration stress. Cell extracts of *E. coli* cultures collected before desiccation (C, control, [log phase]), after 4 h of desiccation (Des) and 40 min of rehydration (Reh) in LB were derivatized with 2,4-dinitrophenylhydrazine (DNPH) for the detection of oxidized proteins. The samples were resolved by SDS-PAGE and immunodetected using anti-DNP antibodies. The relative level of DNP was quantified by densitometry using ImageJ. Error bars represent the standard deviation of three values. Statistical significance was determined by two-way ANOVA with Tukey's test for multiple comparisons (*P < 0.05; **P < 0.01; ***P < 0.001).

In contrast to protein oxidation, lipid peroxidation was inhibited by carnosine (**Figure 6**). In the absence of carnosine, elevated lipid peroxidation after desiccation (~1.4-fold, **) and rehydration (~1.3-fold, **) was detected, possibly due to elevated ROS levels and disrupted membrane integrity. In the presence of carnosine, the TBARS level remained stable and was comparable to the basal TBARS level in the control culture without carnosine.

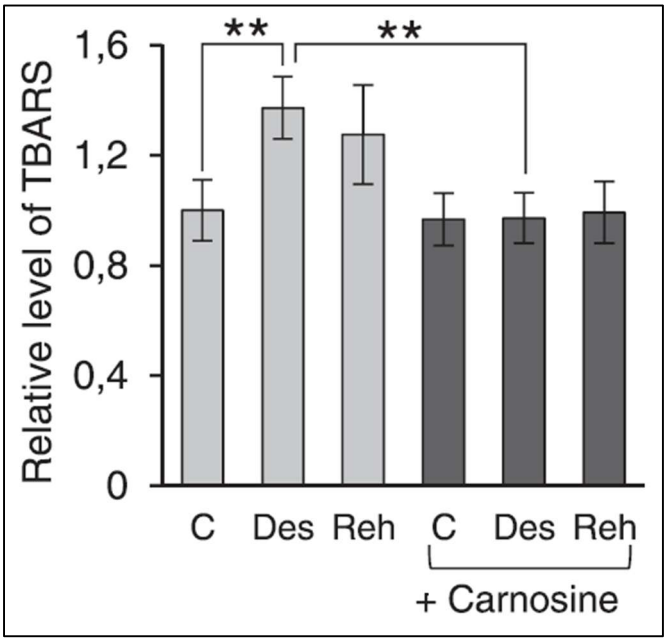

Figure 6. The influence of carnosine on lipid peroxidation in *E. coli* cells exposed to desiccation-rehydration stress. The TBARS assay (was used to quantify lipid oxidation in cell extracts of *E. coli* cultures before desiccation (C-control, log phase) after 4 h of desiccation (Des) and 40 min of rehydration (Reh) in LB. Error bars represent the standard deviation of three values. Statistical significance was determined by two-way ANOVA with Tukey's test for multiple comparisons (*P < 0.05; **P < 0.01; ***P < 0.001).

In conclusion, these results (summarized in **Table 19**) demonstrated that carnosine can protect *E. coli* during desiccation-rehydration stress by preventing the formation of protein aggregates, glycation products and lipid peroxides.

Table 19. Carnosine protects *E. coli* during desiccation-rehydration stress. Summary of results presented in **Figures 1–6**.

	Desiccation		Rehydration	
	–	Carnosine 0.45%	–	Carnosine 0.45%
Culturable cells	17%	15%	30%	40%
VBNC cells	30%	60%	12%	30%
Dead cells	53%	20%	58%	30%
Aggregates	0.7%	0.2%	2.2%	1.2%
Fluorescent AGEs (AU)*	41–11	22–1	35–2	34–1
CML (relative level)	1.6	1.1	1.8	1.2
TBARS (relative level)	1.4	1	1.3	1

* The range of arbitrary units (a.u.) for all six fluorescent products shown in **Figure 3**.

IV.1.5 OM protein OmpC is one of the most glycated proteins in *E. coli*

Immunodetection of CML in *E. coli* extracts revealed that one of the proteins, which corresponded to the ~36 kDa band, was particularly strongly glycated (**Figure 7**). Previous studies (Łupkowska et al., 2023) suggested that the protein is soluble and does not accumulate in protein aggregates. It should be noted that during the isolation of aggregates membranes are solubilized, and all membrane proteins are transferred to the soluble fraction. Therefore, to check whether the 36 kDa protein is a membrane or cytoplasmic protein, the OM was isolated and resolved by gel electrophoresis (**Figure 7 A**). Immunodetection indicated that the 36 kDa protein is one of the OM proteins OmpC or OmpF. Urea gel electrophoresis allowed the clear separation of *E. coli* porins: OmpC, OmpF and OmpA where each of these proteins could later be blotted against CML (**Figure 7 B**). Under control conditions, baseline CML levels are observed, with OmpC exhibiting a relative intensity of approximately 1.0 and OmpF at around 0.4 (**Figure 7 C**), suggesting minimal constitutive modification in unstressed cells. Desiccation induces a marked elevation in CML for OmpC, reaching ~1.8, while OmpF shows a modest increase to ~0.9 without noted significance. Upon rehydration, CML levels in OmpC further escalate to ~2.2, indicating that the reintroduction of hydration exacerbates or sustains these modifications, possibly through rehydration-associated oxidative bursts or incomplete refolding. In contrast, OmpF remains at ~1.0,

underscoring a porin-specific response where OmpF's narrower pore or differential regulation might confer resistance to CML accumulation. Interestingly, CML was not detected in OmpA, in contrast to OmpC and OmpF.

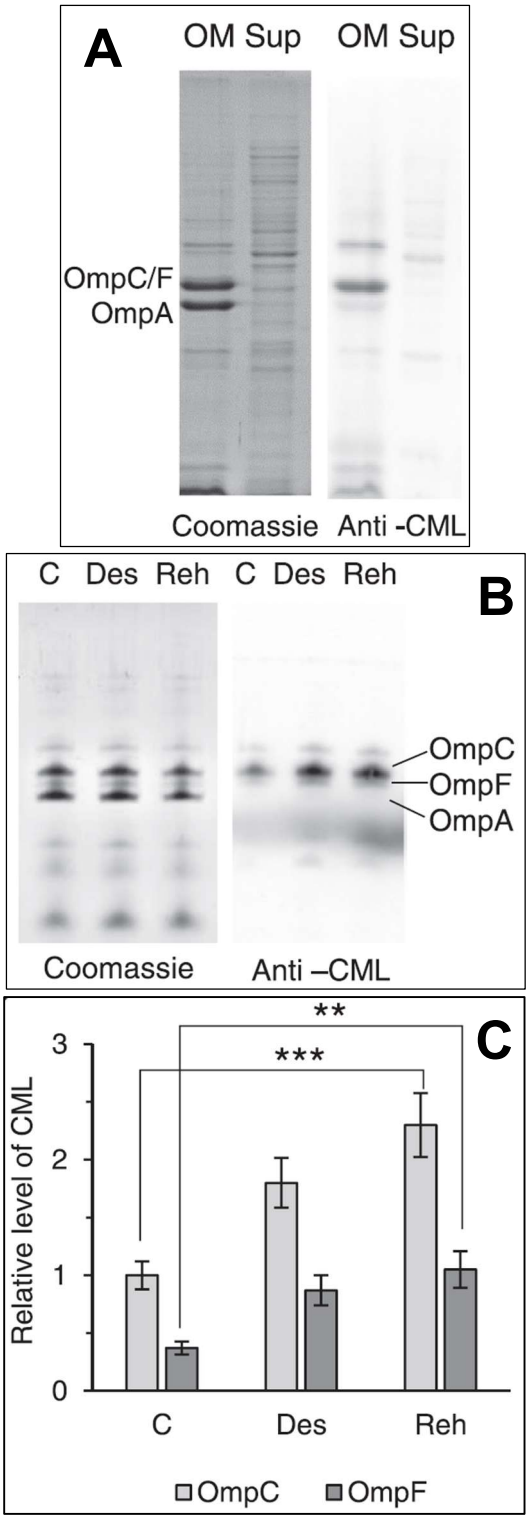

Figure 7. Identification of glycated proteins in the outer membrane (OM) of *E. coli*; **A)** The OM was isolated from an exponential *E. coli* culture as described in Material and Methods. The OM and the remaining proteins collected in the supernatant were subjected to SDS-PAGE and Coomassie staining or immunodetection with anti-CML antibodies; **B)** To separate OmpC and OmpF, the OM proteins were resolved by urea gel electrophoresis. The samples were collected from the control culture, after 4 h desiccation (Des) and 40 min rehydration (Reh); **C)** The relative levels of glycated OmpC and OmpF normalized to protein concentration were estimated by densitometry and ImageJ. Representative gels and immunoblots from three independent experiments are shown. Error bars represent the standard deviation of three values. Statistical significance was determined using one-way ANOVA with Tukey's multiple-comparison test (*P < 0.05; **P < 0.01; ***P < 0.001).

IV.1.6 Effects of betaine, carnosine and trehalose on *E. coli* viability, protein aggregation and accumulation of glycation products during long-term desiccation

Bacteria accumulate compatible solutes, such as betaine and trehalose, as a key mechanism to mitigate osmotic stress and desiccation (Burgess and Huang, 2016; Laskowska and Kuczyńska-Wiśnik, 2020). These osmoprotectants function as chemical chaperones by stabilizing proteins and promoting their refolding. However, their potential anti-glycation properties remain poorly understood. As a non-reducing sugar, trehalose avoids participating in Maillard reactions with amino groups and may inhibit glycation through protein stabilization. In prior work, it was shown that low concentrations (<0.4%) of trehalose and betaine suppressed protein aggregation during the stationary phase, whereas higher concentrations of these osmolytes promoted aggregation (Leszczynska et al., 2013). Therefore, in the next experiment, different concentrations of carnosine, betaine and trehalose were used to check if there is any relationship between the levels of aggregates or AGEs and *E. coli* survival during long-term desiccation (20 h). It was found that lower (0.2 %) and higher (0.45 %) concentrations of carnosine inhibited the formation of aggregates and AGEs (**Figure 8 A**, **B**) and improved *E. coli* survival (**Figure 8 C**). The amount of dead and culturable cells were significantly ($p < 0.05$) decreased and increased, respectively (**Figure 8 C**). In the presence of 0.2 % betaine, protein aggregation was strongly inhibited (**Figure 8 A**), but glycation and culturability were not affected. 0.45 % betaine caused massive aggregation of proteins (**Figure 8 A**) but prevented AGEs formation and enhanced survival. In the presence of 0.2% trehalose the level of protein aggregates decreased,

while 0.45 % trehalose led to enhanced aggregation. However, regardless of the concentration, trehalose inhibited glycation and improved survival.

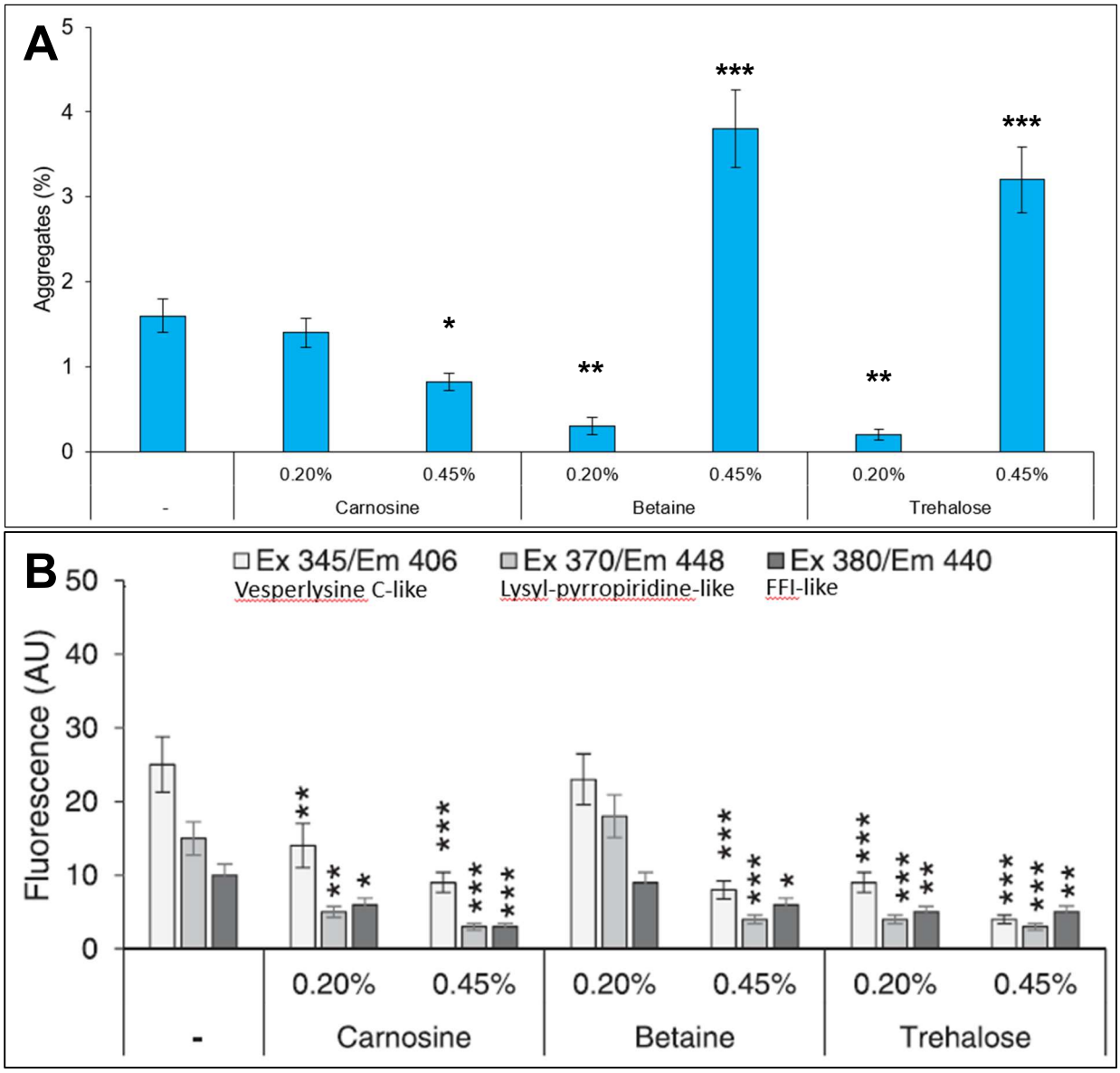

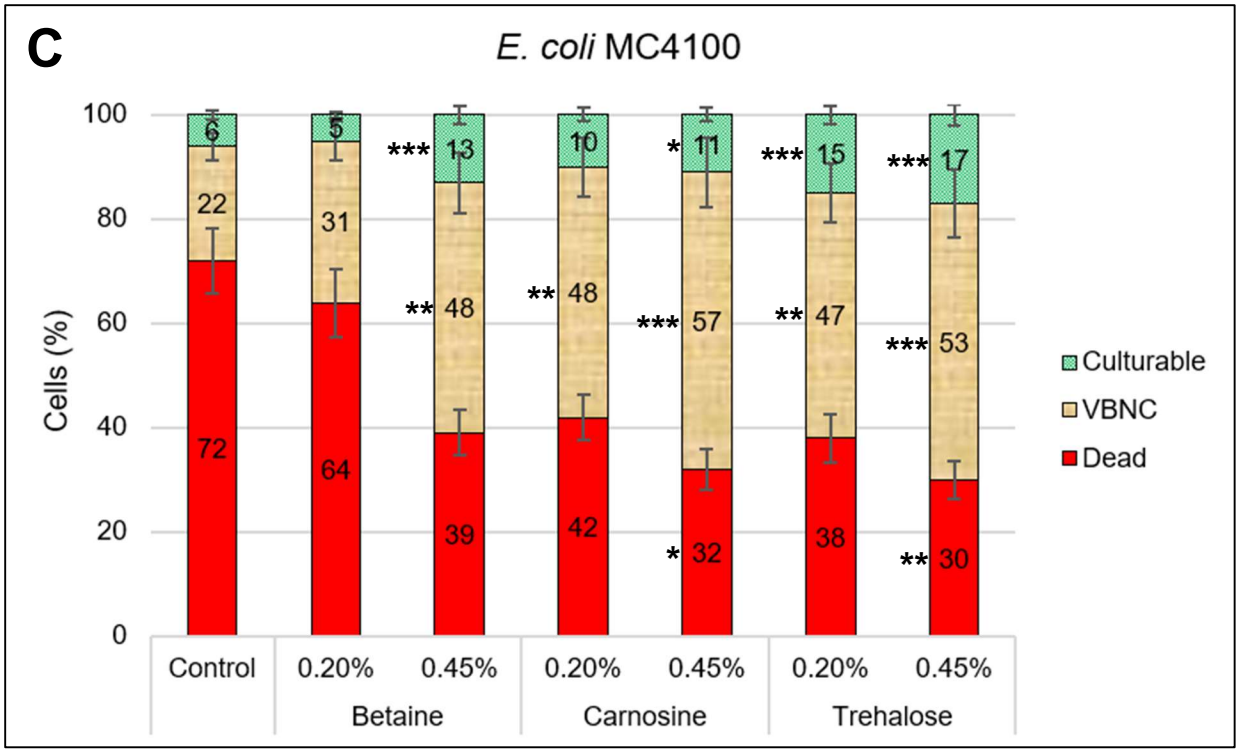

Figure 8. *E. coli* aggregate formation, glycation and viability during long-term desiccation (20 h); **A)** Protein aggregates were isolated, resolved by SDS-PAGE and analysed by densitometry after Coomassie staining (100 % -total protein in the extracts); **B)** Fluorescence values specific for: vesperlysine C-like (Ex 345 nm/ Em 404 nm), lysyl-pyrropiridine-like (Ex 370 nm/ Em 448 nm) and FFI-like (Ex 380 nm/ Em 440 nm) products; **C)** The percentage of culturable, nonculturable and dead cells in *E. coli* populations was estimated as described in III.3 Error bars represent the standard deviation of three values. Statistical significance was determined using one-way ANOVA with the Tukey's multiple-comparison test (*P < 0.05; **P < 0.01; ***P < 0.001). The asterisks represent statistical differences between the control (-) and carnosine-, betaine- or trehalose-treated cultures.

In summary, these experiments indicated that glycation, rather than protein aggregation, was the primary cause of the loss of cell viability under desiccation stress.

IV.1.7 Lysine acetylation ameliorates protein glycation *in vivo* and *in vitro*

Because glycation and acetylation both target lysine residues, they appear to compete. For example, lysine acetylation has been shown to protect histones from harmful glycation in a breast cancer cell line (Zheng et al., 2019). Additionally, Nε-lysine acetylation and AGE formation were found to co-occur in the eye lens molecular chaperones αA- and αB-crystallin (Nahomi et al., 2013). Pre-acetylation of αA- and αBcrystallin *in vitro* before glycation with MGO significantly reduced AGE synthesis. To

determine whether similar effects occur in *E. coli* proteins, whole cell extracts from the *E. coli ΔackA-pta* strain were incubated at 37 ℃ with or without 10 mM acetylphosphate (AcP) for 5 days to trigger glycation. AcP is a source of acetyl groups for spontaneous lysine acetylation both in *vivo* and *in vitro*. The *ΔackA-pta* strain is unable to synthesize AcP (**Figure 9**) and was used to minimize the initial level of acetylation in the extract.

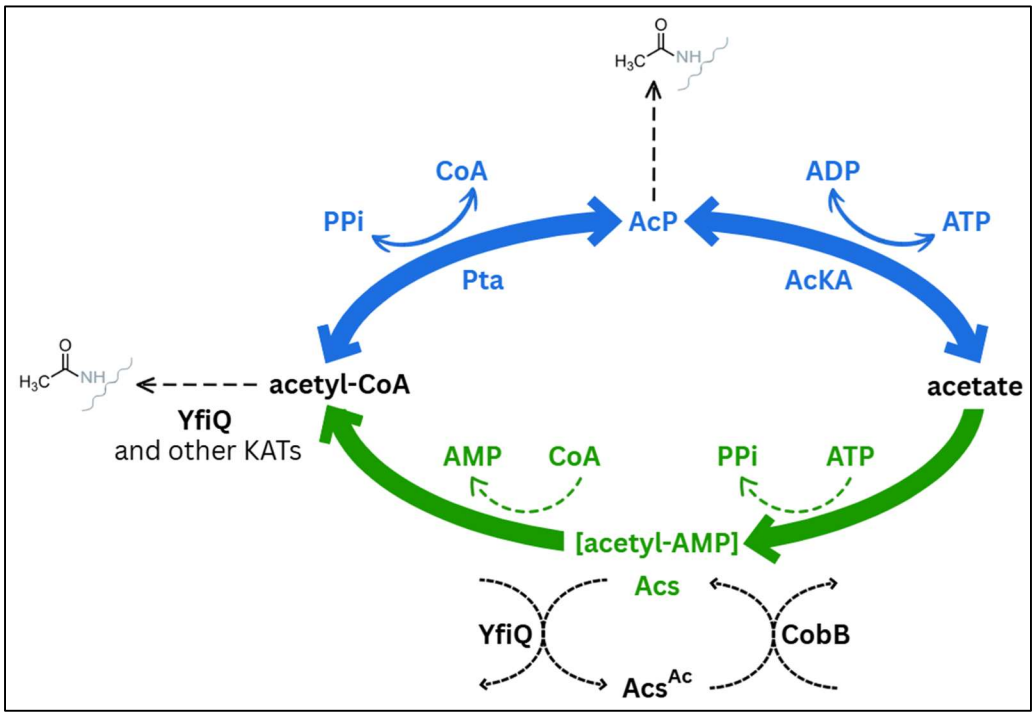

Figure 9. Nε-lysine acetylation pathways in *E. coli*. The nonenzymatic AcP-dependent and KATs-dependent pathways are responsible for protein acetylation. KATs use acetyl-CoA as a donor of the acetyl group. AckA, acetate kinase; AcP, acetyl phosphate; Acs, acetate-CoA ligase; CobB, NAD-dependent protein-lysine deacetylase; KATs, lysine acetyltransferases; Pta, phosphotransacetylase; YfiQ, protein lysine acetyltransferase.

After incubation at 37 ℃, the samples were resolved by SDS-PAGE and immunodetected using anti-acetyl lysine (anti-AcK) and anti-CML antibodies (**Figure 10**).

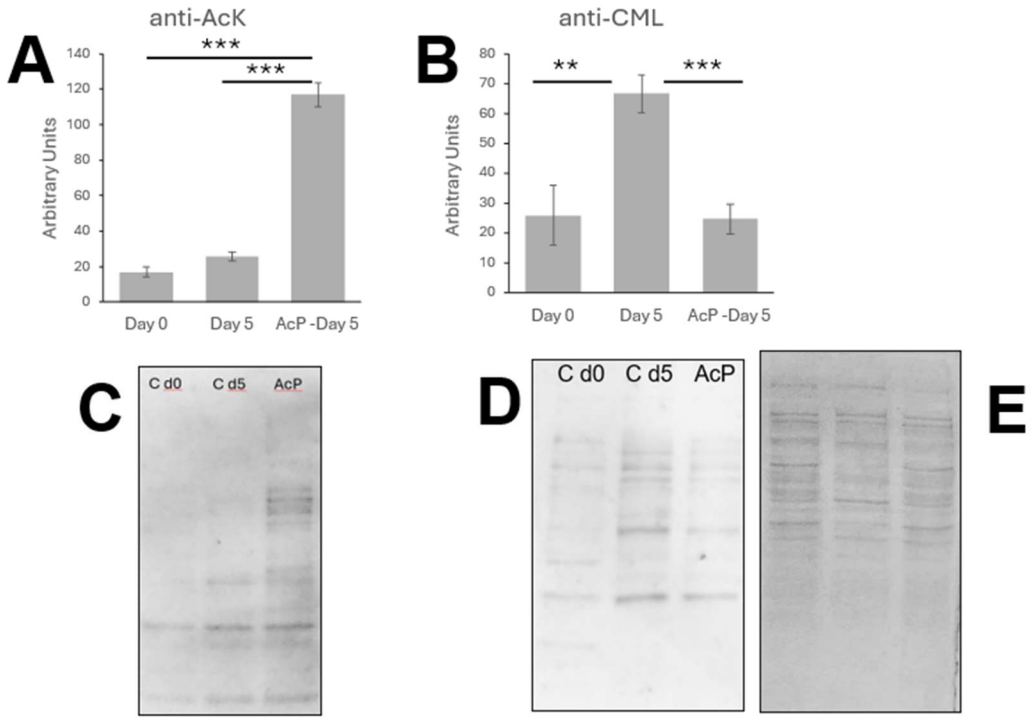

Figure 10. AcP-dependent acetylation inhibits formation of CML in *in vitro E. coli* Δ*ackA-pta* extracts. *E. coli* Δ*ackA-pta* extracts were prepared as described in the Materials and Methods section. The extracts were supplemented with or without 10 mM AcP and incubated at 37 ℃. The samples taken at day 0 (before incubation at 37 ℃) and after 5 days of incubation were resolved by SDS-PAGE and immunodetected with anti-AcK (**A**, **C**) and anti-CML antibodies (**B**, **D**); **E)** The Coomassie-stained gel; **A**, **B)** The relative levels of AcK and CML were quantified by densitometry using ImageJ. Statistical significance was determined using one-way ANOVA with Tukey's multiple-comparison test (*P < 0.05; **P < 0.01; ***P < 0.001).

Significant acetylation of *E. coli* proteins was observed in the presence of AcP (**Figure 10 A**, **C**). Incubation of the extracts at 37°C resulted in enhanced glycation (>2-fold increase in CML levels compared to day 0) only in the sample without AcP (**Figure 10 B**, **D**). Therefore, these results showed that non-enzymatic lysine acetylation by AcP inhibited the accumulation of CML *in vitro*.

Further experiments demonstrated that samples incubated at 37 ℃ for 5 days exhibited a strong fluorescence peak at 450 nm (excitation at 350 nm), indicating the presence of fluorescent AGEs (**Figure 11**) However, the formation of fluorescent products was significantly inhibited in the presence of AcP.

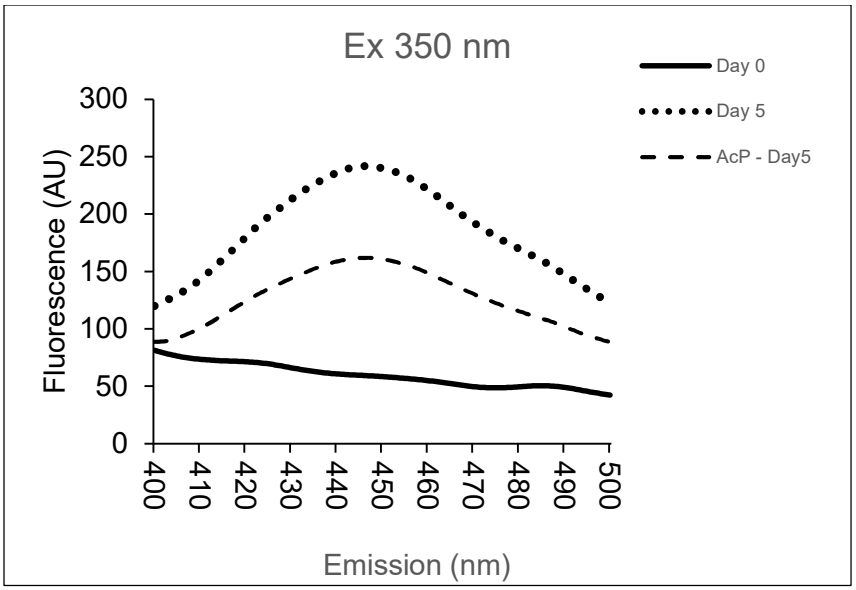

Figure 11. AcP-dependent acetylation inhibits formation of fluorescent AGEs in *E. coli* Δ*ackA-pta* extracts. *E. coli* Δ*ackA-pta* extracts obtained in the previous experiment (**Figure 10**) were used to determine the level of fluorescent AGEs (Ex 350 nm / Em 450).

Taken together, these results confirmed that lysine acetylation may prevent protein glycation *in vitro.* To determine whether a similar effect occurs *in vivo*, AcK and AGEs levels were estimated in *E. coli* Wild Type (WT) and acetylation-deficient strains exposed to desiccation-rehydration stress (**Figure 12**). Since Δ*ack-pta* cells exhibited an initial acetylation level comparable to that of the WT strain (data not shown), a triple Δ*ack-pta-pka* mutant was tested to completely halt lysine acetylation (**Figure 9**). In the *Δack-pta-pka* strain, despite the absence of the *ack-pta* pathway and the acetyltransferase Pka, increased AcK levels have been detected after desiccation and rehydration compared to the control (before desiccation). Nevertheless, the level of acetylation was significantly lower in the Δ*ack-pta-pka* strain than in WT cells (**Figure 12 A**). Notably, reduced lysine acetylation in the mutant strain was associated with increased accumulation of AGEs (**Figure 12 B**). Therefore, these results confirmed that lysine acetylation may prevent its glycation also *in vivo*.

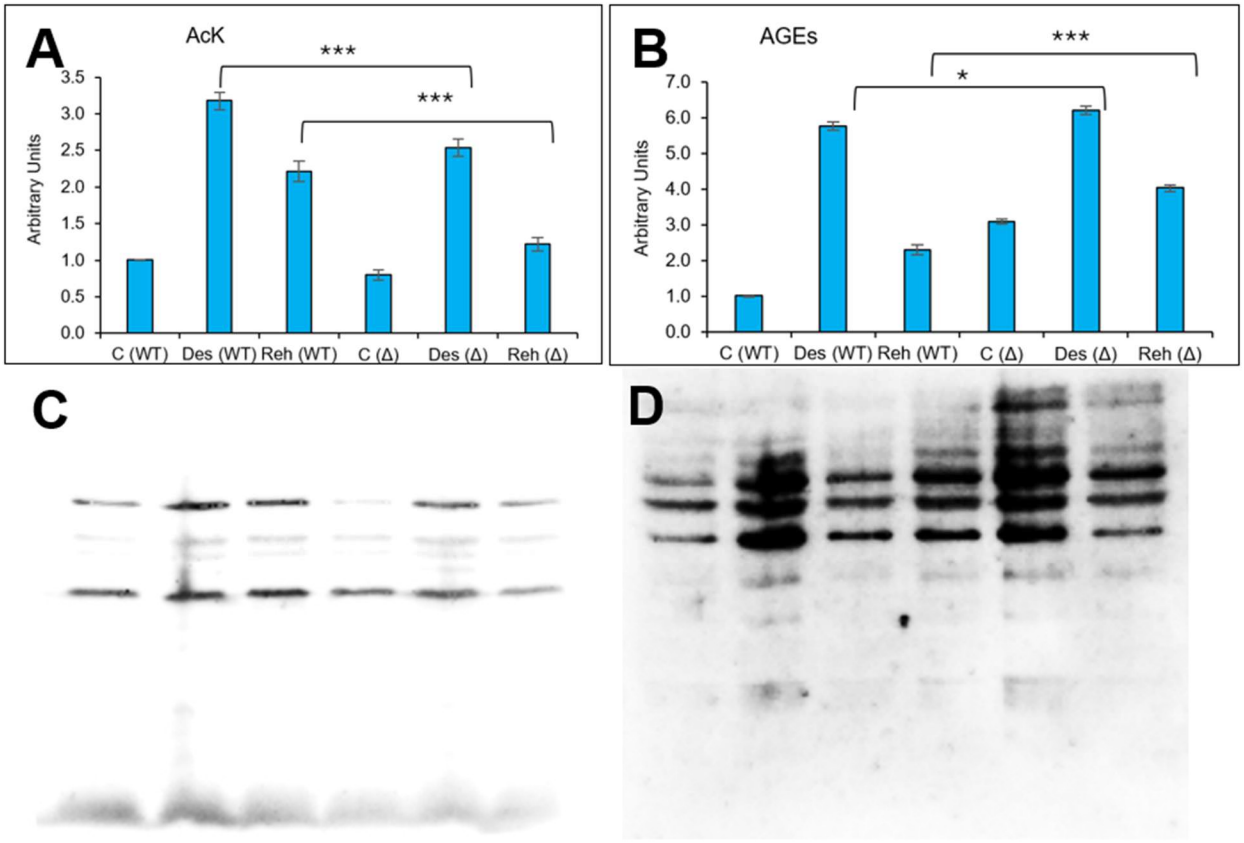

Figure 12. Lysine acetylation inhibits CML formation in *E. coli* Δ*ackA-pta-pka* cells exposed to desiccation-rehydration stress. *E. coli* WT and Δ*ackA-pta-pka* strains were grown in LB to an OD_{595} of 0.5 (C, control), then exposed to 4 h of desiccation (Des), followed by 40 min of rehydration (Reh); Bar graphs in a.u. show **A)** lysine acetylation and **B)** lysine glycation, as detected by anti-AcK and anti-AGE antibodies, respectively. Graphs were generated using densitometry in ImageJ. Error bars represent the standard deviation of three values. Statistical significance was determined by one-way ANOVA with Tukey's test for multiple comparisons (*P < 0.05; **P < 0.01; ***P < 0.001). Representative nitrocellulose membranes (**C**, **D**) from three independent experiments are shown. 10 µg of protein was loaded onto each lane.

Enhanced glycation in Δ*ackA-pta-pka* cells was associated with decreased culturability and viability compared to the WT strain (**Table 20**). Although the differences were rather mild, this tendency was observed both after desiccation and rehydration. The results agree with the assumption that *E. coli* survival depends on the extent of glycation.

Table 20. Comparison of viability and culturability of *E. coli* BW25113 WT and Δ*ackA-pta-pka* cells exposed to desiccation-rehydration stress.

	WT		Δ*ackA-pta-pka*	
Cells (%)	Des	Reh	Des	Reh
Culturable	15 ± 3	26 ± 2	11.5 ± 1.5	19.5 ± 0.5
VBNC	35.5 ± 1.5	24.5 ± 2.5	30 ± 1	25 ± 1
Dead	49.5 ± 4.5	49.5 ± 0.5	58.5 ± 2.5	55.5 ± 0.5

IV.2 Influence of betaine, carnosine and trehalose in viability, the formation of protein aggregates and glycation products in *K. pneumoniae*

Further experiments were conducted on *K. pneumoniae* MKP103 to examine whether the observed relationship between viability, aggregate formation, and glycation products in *E. coli* also occurs in other bacterial species. An initial set of four experiments was conducted on *K. pneumoniae* MKP103 in Neidhardt MOPS minimal medium (NMMM) to assess the protective effects of various osmolytes in a chemically defined environment. These experiments comprised four primary assays i) growth rate analysis, (ii) live/dead cell staining for viability assessment, (iii) aggregate quantification, and (iv) persister cell formation.

However, the high buffering capacity of NMMM was observed to maintain homeostasis, thereby preventing the formation of glycation products, subsequent protein aggregates, and persister cells. Consequently, to elicit and study these specific stress-related phenomena, the entire experimental series was subsequently repeated using the nutritionally rich LB medium.

IV.2.1 Effects of betaine, carnosine and trehalose on *K. pneumoniae* viability, protein aggregation and accumulation of glycation products

After desiccation, the betaine-treated sample showed a lower percentage of dead cells (29.9%) compared to the control (35.4%). This protection came from shifting cells into a dormant VBNC state. The betaine sample had more VBNC cells (69.7%) than the control (63.8%). Interestingly, the control group retained a slightly higher percentage of live, culturable cells (0.8%) compared to the betaine group (0.5%). This suggests that

while betaine prevented outright death, it pushed more cells—including some that were initially culturable—into the VBNC state. This confirms betaine's role as an osmoprotectant that favors cell preservation in a non-culturable, dormant state over immediate death. Upon rehydration, the trend reversed for the bulk population. The betaine group now had a much higher percentage of dead cells (41.2%) than the control (33.6%). This mass death comes from the VBNC population, which drops from 69.7% to 58.4%. The most striking new finding was in the live population. The betaine-treated cells retained a higher percentage of culturable cells (0.4%) post-rehydration compared to the control, which crashes to just 0.1%. This reveals two opposing fates within the betaine-treated sample. For the vast majority (the VBNC population), rehydration was catastrophic. For the tiny sub-population of culturable cells, betaine provides a significant survival advantage during the shock of rehydration, helping them remain culturable.

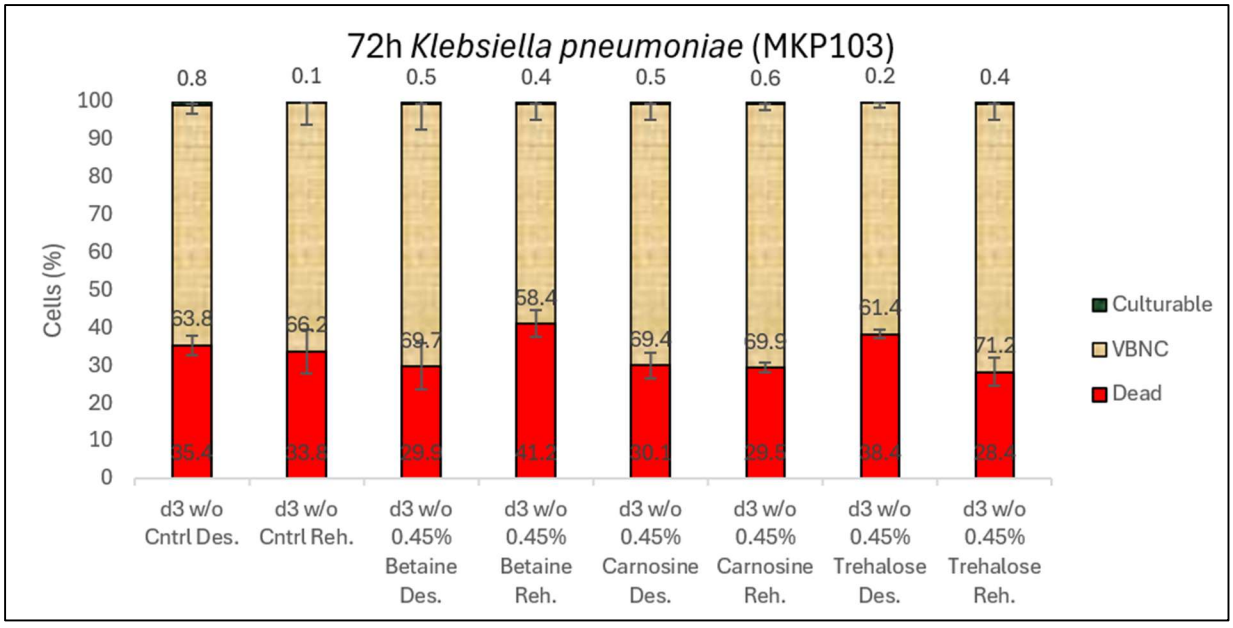

Figure 13. Influence of osmolytes on *K. pneumoniae* MKP103 culturability under desiccation-rehydration stress. *K. pneumoniae* MKP103 was grown in LB supplemented or not with 0.45% betaine, carnosine, and trehalose to an OD_{595}= 0.5 (Cntrl). The cultures were exposed to desiccation for 72 h (Des) followed by 40 min rehydration (Reh). The percentages of culturable, VBNC, and dead cells were estimated as described in section III.3. Error bars represent the standard deviation of three values.

During the 72-hour drying period, carnosine clearly demonstrates a protective effect compared to the control. The carnosine-treated sample had significantly fewer

dead cells (30.1%) than the control group (35.4%). This increased survival is attributed to more cells entering a VBNC state, with the carnosine group showing 69.4% VBNC versus 63.8% in the control. Similar to the previous experiment, the control group retained a slightly higher percentage of initially culturable cells (0.8%) compared to the carnosine group (0.5%), suggesting carnosine also promotes entry into the VBNC state for maximum preservation. Carnosine's protective qualities persist and become even more apparent during the critical rehydration stage. Unlike betaine in the previous analysis, carnosine continues to protect cells. The rehydrated carnosine sample had the lowest percentage of dead cells (29.5%) of any condition, which is better than the rehydrated control (33.6%). Carnosine dramatically aided the recovery of culturable cells. The live population in the carnosine group was 0.6%, which is six times higher than the control group's mere 0.1%. This shows carnosine not only prevents death but actively supports the return to a culturable, reproductive state.

Surprisingly, and in contrast to the other osmolytes, trehalose appears to be ineffective or even slightly detrimental during the 72-hour drying process. The trehalose-treated sample showed a higher percentage of dead cells (38.4%) compared to the untreated control (35.4%). Consequently, both the VBNC: 61.4% and culturable (0.2%) populations were smaller than in the control sample (VBNC: 63.8%, Culturable: 0.8%). This indicates that during the stress of drying itself, trehalose did not confer a survival advantage. The protective properties of trehalose become evident only upon rehydration, where it provides a substantial survival benefit. After rehydration, the trehalose group had the lowest percentage of dead cells (28.4%) seen in the experiment, a significant improvement over the rehydrated control (33.6%). Trehalose substantially aided the recovery of culturable cells. The live population in the trehalose group was 0.4%, which is four times higher than the control group's 0.1%. It also maintained the highest percentage of VBNC cells at 71.2%.

The desiccated control sample exhibits a baseline aggregate percentage of 3.9%, indicative of minimal protein misfolding or aggregation induced by desiccation alone in the absence of osmolytes. Upon rehydration, this value decreases slightly to 3.4%, suggesting that rehydration may partially alleviate desiccation-induced stress

without significant aggregate resolubilization or degradation in untreated cells. In contrast, supplementation with 0.2% betaine markedly elevates aggregate formation, yielding 22.6% in desiccated samples—a 5.8-fold increase over the control—and further escalating to 26.3% upon rehydration, representing a 7.7-fold increase relative to the rehydrated control. This pattern implies that betaine at 0.2% not only promotes aggregate stabilization during water loss but may exacerbate aggregation during the rehydration phase, potentially through mechanisms involving altered protein-solvent interactions or chaperone overload, as osmolytes like betaine are known to preferentially exclude water from protein surfaces, thereby influencing folding landscapes (Łupkowska et al., 2023). At the higher concentration of 0.45% betaine, aggregate percentages remain elevated but show a tempered response: 20.4% in desiccated samples (5.2-fold over control) and 19.2% in rehydrated samples (5.6-fold over control). Notably, while desiccation under 0.45% betaine induces aggregates comparable to 0.2% (20.4% vs. 22.6%), rehydration results in a lower aggregate burden (19.2% vs. 26.3%), suggesting a potential threshold effect where higher betaine levels confer partial protective benefits during recovery, possibly by enhancing cellular osmoadaptation or modulating aggregate dissolution pathways.

Supplementation with 0.2% carnosine substantially amplifies aggregation, registering 25.9% in desiccated samples (a 6.6-fold elevation over control) and 26.3% in rehydrated samples (7.7-fold over control). This escalation during rehydration suggests carnosine may hinder aggregate resolubilization, possibly by altering hydration shells or overwhelming chaperone systems during osmotic recovery. At 0.45% carnosine, aggregates further intensify to 26.6% in desiccation (6.8-fold increase) and 27.8% in rehydration (8.2-fold increase), indicating a concentration-proportional augmentation without the threshold attenuation seen in other osmolytes.

These patterns diverge from betaine's effects in analogous *K. pneumoniae* setups, where 0.2% betaine yielded 22.6% (desiccated) and 26.3% (rehydrated) aggregates, but 0.45% moderated rehydration aggregates to 19.2%, implying betaine's preferential exclusion mechanism may afford better recovery at higher doses compared to carnosine's histidine-β-alanine structure, which could favor histidine-mediated

interactions promoting stable aggregates. This aligns with findings in *E. coli*, where high concentrations of glycine betaine and trehalose enhanced protein aggregation during desiccation-rehydration while inhibiting glycation, potentially as an adaptive response sequestering vulnerable proteins and bolstering survival.

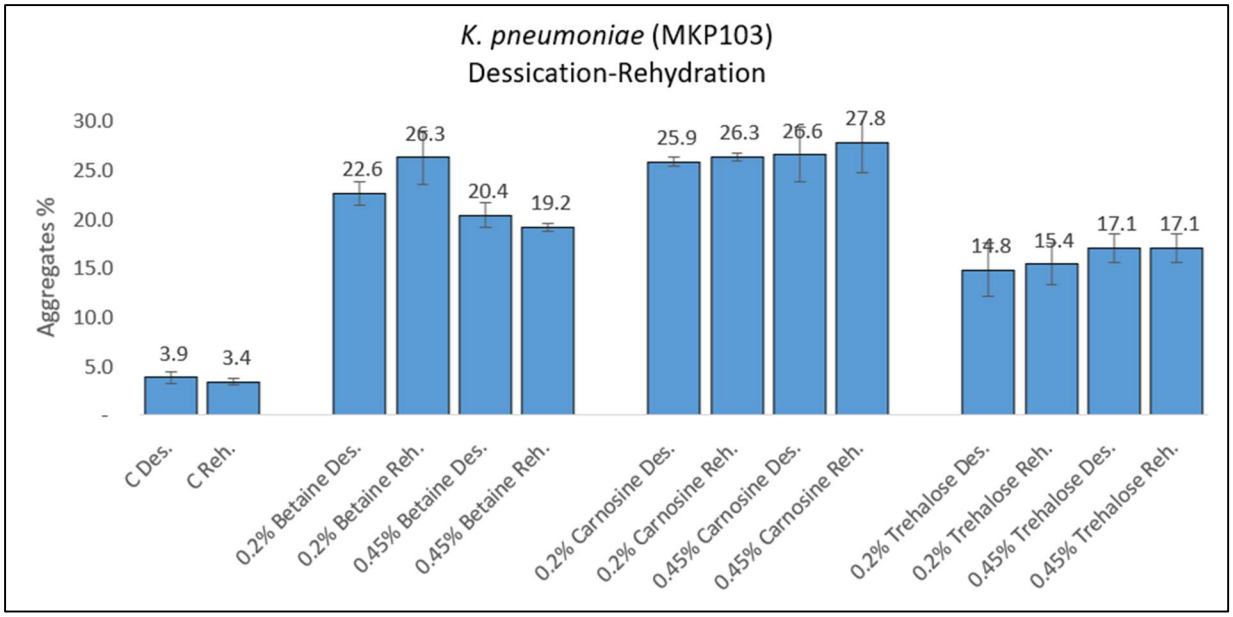

Figure 14. Influence of osmolytes on the formation of protein aggregates in *K. pneumoniae* MKP103 under desiccation-rehydration stress. Protein aggregates were isolated as described in the Materials and Methods section. The aggregates and whole cell extracts were resolved by SDS-PAGE and stained with Coomassie, then analyzed by densitometry using ImageJ software. Error bars represent the standard deviation of three values.

Introduction of 0.2% trehalose elevates aggregates to 14.8% during desiccation (3.8-fold versus control) and 15.4% upon rehydration (4.5-fold), indicating moderate promotion of aggregate accrual that persists through recovery phases. At 0.45% trehalose, aggregation intensifies to 17.1% in both desiccated and rehydrated states (4.4-fold and 5.0-fold over respective controls), evincing a concentration-dependent escalation without rehydration-mediated alleviation, potentially attributable to trehalose's vitrification properties fostering stable, protective aggregates.

Trehalose profile contrasts with betaine and carnosine counterparts in *K. pneumoniae* MKP103, where 0.2% betaine induced higher aggregates (desiccated: 22.6%; rehydrated: 26.3%) and 0.45% betaine exhibited rehydration attenuation

(19.2%), while carnosine yielded the most pronounced aggregation (0.2% : 25.9% / 26.3%; 0.45% : 26.6% / 27.8%). Trehalose's comparatively subdued induction—averaging ~16% across conditions—suggests superior stabilization efficacy, possibly via water-replacement mechanisms despite elevated glycation levels while permitting controlled aggregation as an adaptive sequestration strategy.

To determine the influence of betaine, carnosine, and trehalose on the AGEs formation, fluorescent AGEs were detected in *K. pneumoniae* MKP103 as in the case of *E. coli* (**Figure 3**). Osmolyte-treated media collectively exhibited elevated levels of cytosolic fluorescent AGEs for both desiccated and rehydrated *K. pneumoniae* cultures (**Figure 15 C**).

The unexpected results were further proof checked by dot-blotting the same whole cell extracts of *K. pneumoniae* MKP103 subjected to desiccation-rehydration stress on nitrocellulose membranes against anti-AGE and Ack antibodies (**Figure 15 D**, **E**). For anti-AGE, the untreated desiccated control induced a high relative AGE level of approximately 1.0 a.u., which decreased to ~0.55 a.u. upon rehydration, indicating partial resolution or dilution of glycative modifications post-stress. All three osmolytes moderately attenuated desiccation-associated AGE accumulation to ~0.80 a.u., with rehydration levels of betaine at ~0.65 a.u. and similar rehydration levels for both carnosine and trehalose at ~0.55 a.u., comparable to control rehydration values.

At this stage, it is difficult to explain discrepancies between these two results: osmolytes-dependent increase of fluorescent AGEs and moderate decrease of AGEs detected by Western blotting (see Discussion).

Assuming that AGE accumulation may be reduced by acetylation, as suggested by previous results in *E. coli* (**Figure 3**), the acetyl-lysine level was also determined. Indeed, increased acetylation was observed in *K. pneumoniae* cultures supplemented with osmolates and exposed to desiccation.

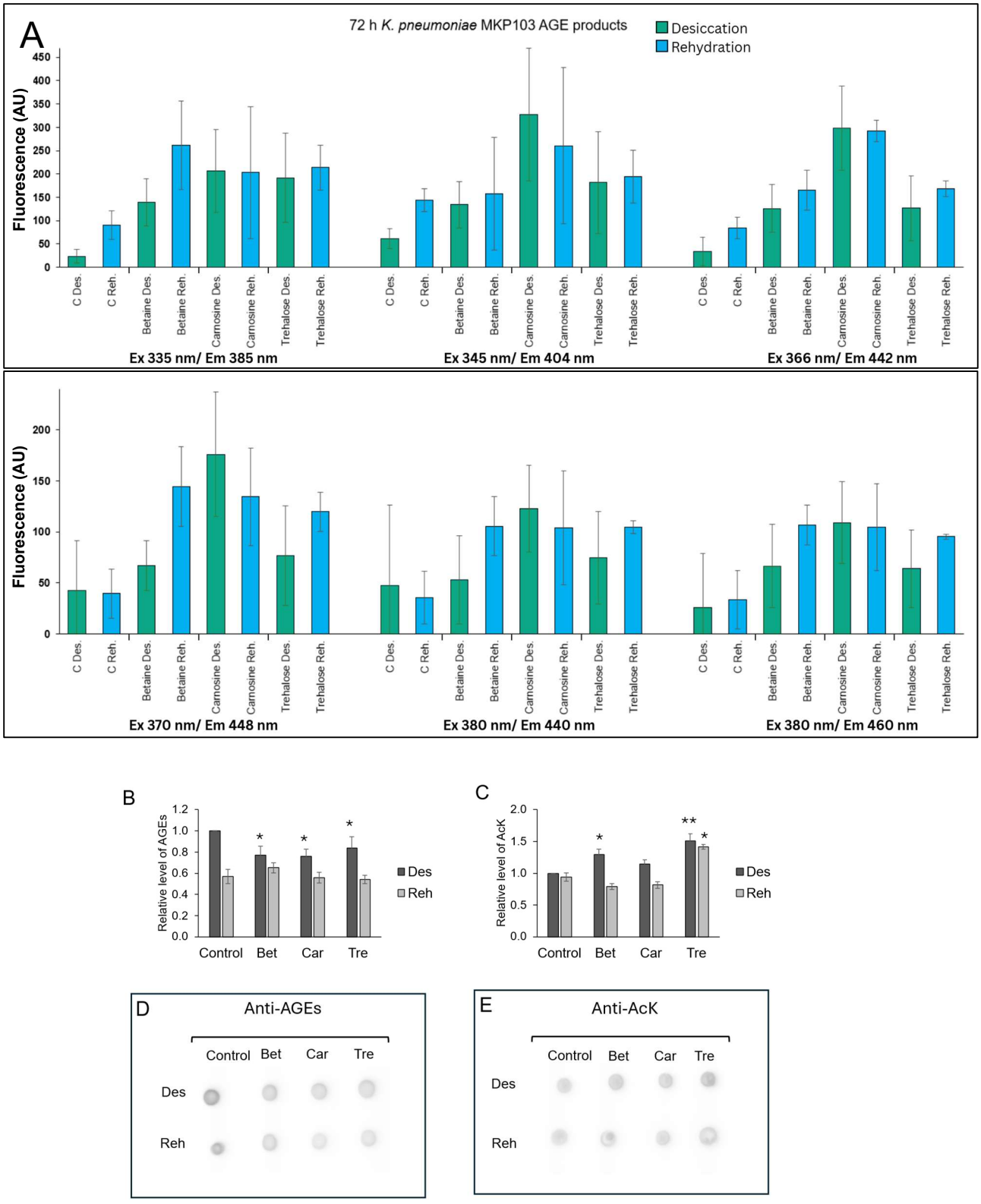

Figure 15. Influence of osmolytes on the formation of glycation products and AcK in *K. pneumoniae* cultures exposed to desiccation-rehydration stress. *K. pneumoniae* MKP103 was grown in LB supplemented or not with 0.45% betaine, carnosine, or

trehalose to an OD_{595}= 0.5 (Control). The cultures were exposed to desiccation for 72 h (Des) followed by 40 min rehydration (Reh); **A)** Six different fluorescence excitation/emission settings correspond to six types of glycation-like products; upper row: Ex 335 / Em 385 (Excitation [Ex.] at 335 nm and emission [Em.] at 385 nm) for pentosidine-like, Ex 345 / Em 406 for vesperlysine C-like, Ex 366 / Em 442 for vesperlysine A/B-like; and lower row: Ex 370 / Em 448 for lysyl-pyrropiridine-like, Ex 380/Em 460 for fluorolink-like, Ex 380 / Em 440 for FFI-like; **B-E)** Effect of osmolytes on the level of AGEs and AcK. Whole cell extracts (4 µg of protein) were dot-blotted on a nitrocelluose membrane and detected using anti-AGEs (**B**, **D**) and anti-AcK antibodies (**C**, **E**); The itensity of spots was quantified by densytometry and used to evaluate the level of AGEs and AcK (**D**, **E**). Representative dot-blots are shown. Error bars represent the standard deviation of three values. Statistical significance was determined using one-way ANOVA with the Tukey's multiple-comparison test (*P < 0.05; **P < 0.01; ***P < 0.001). The asterisks represent statistical differences between the control and carnosine-, betaine- or trehalose-treated cultures.

IV.2.2 The center and ring subpopulations in macrocolonies of *K. pneumoniae* 577-BA clinical isolate

Another model used to investigate the effects of desiccation stress on viability, protein aggregation, and glycation in bacterial cells was macrocolonies formed by the *K. pneumoniae* clinical isolate 577-BA. 577-BA forms macrocolonies on solid media that differentiate during growth into the mucoid center and non-mucoid ring (**Figure 16**).

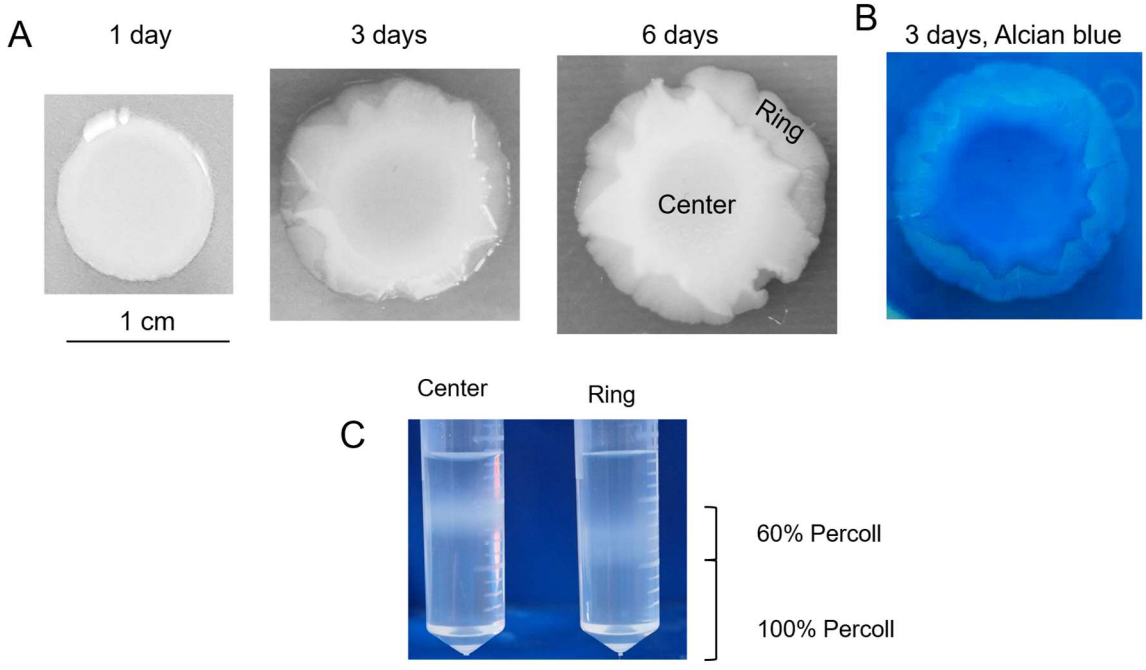

Figure 16. Differentiation of BA-577 macrocolonies into a mucoid (capsulated) center and a non-mucoid (non-capsulated) ring during growth; **A)** 10 µl of overnight BA-577 cultures were spotted on LA plates and incubated at 37 ℃ for 6 days; **B)** Alcian blue

staining of a 3-day macrocolony indicates the presence of capsular polysaccharides in the center; **C)** Suspensions of bacteria (0.5 mL; OD_{595} = 0.3, PBS) collected from the center and ring were layered on a top of the two step Percoll gradient (1 mL of 100% and 0.5 mL of 60% Percoll in PBS). The samples were centrifuged at 1 400 × g for 5 min at room temperature.

The presence of a capsule in the center was confirmed by staining macrocolonies with the cationic dye Alcian blue, which detects acidic polysaccharides (**Figure 16 B**), and centrifugation of the subpopulations in a Percoll-density gradient (Nunez et al., 2023) (**Figure 16 C**). Capsule-deficient bacteria from the ring migrated throughout the 60%, while the capsulated cells from the center remained at the top of the 60% layer.

The transition from mucoid (capsulated) to non-mucoid (non-capsulated) phenotype has been previously reported in clinical carbapenemase-producing *K. pneumoniae* strains by Chiarelli et al. (2020). The loss of the mucoid phenotype correlated with capsule deficiency and resulted from transposon insertions or point mutations in the capsule operon. The capsule is a major virulence factor and protects bacteria against biotic and abiotic stresses, including the host immune system, bacteriophages, and desiccation (Buffet et al., 2021). Therefore, it was expected that prolonged incubation of macrocolonies would lead to faster desiccation and damage accumulation in the non-capsulated subpopulation.

However, the addition of the osmolytes under investigation (carnosine, betaine and trehalose) inhibited the development of this differentiated morphology (**Figure 17**). Cultures supplemented with these compounds failed to form the characteristic, well-separated ring and center structures. Consequently, all subsequent investigations of macrocolony spatial differentiation—including viability staining, aggregate analysis, and AGE detection—were necessarily performed in the absence of exogenous osmolytes. Unlike the control where a discernable miniscule between the ring and center subpopulations is vsibile, macrocolonies of *K. pneumoniae* (BA-577) under the influence of applied osmolytes did not produce such result. That made it difficult to proceed with separation of ring subpopulation therefore aggregate extraction.

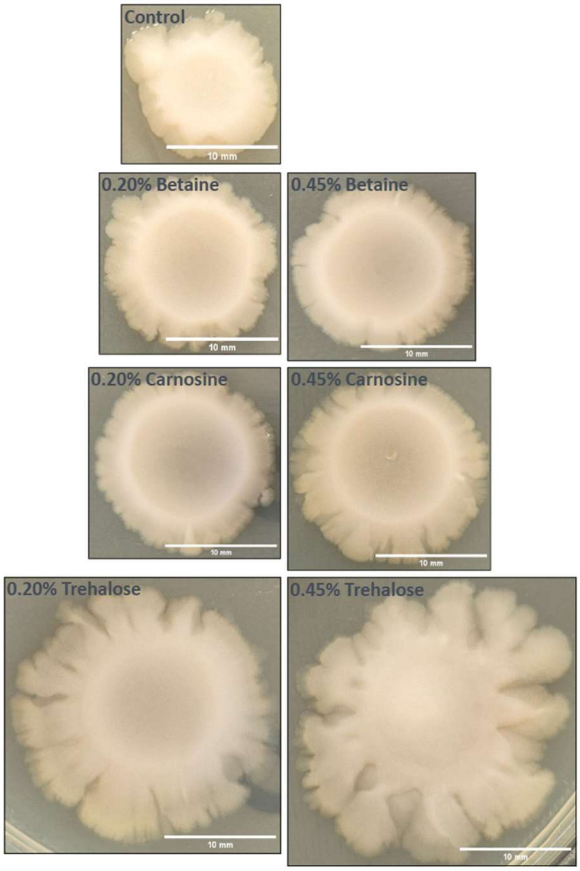

Figure 17. Ring and center subpopulations morphology of 5-day old macrocolonies of *K. pneumoniae* 577-BA under the unfluence of 0.2% and 0.45% betaine, carnosine, and trehalose, grown at 37 ℃.

The subpopulations of the BA-577 have been partially characterized (Łupkowska, 2025). Differences in viability, the proteomes and antibiotic tolerance have been observed between the center and ring subpopulations isolated from 3-day microcolonies (**Table 21**). However, the extent of protein aggregation in both subpopulations remained unknown.

Table 21. Differences between the C and R subpopulations in BA-577 3-day macrocolonies (Łupkowska, 2025)

	Center (C)	Ring (R)
Live cells (%)	3	11
Dead cells (%)	9	11
VBNC (%)	88	78
Calcofluor binding (cellulose production)	+	–
Protein aggregates	?	?
CML (immunodetection, A.U.) AGEs (immunodetection, A.U.)	2.5 2.4	0.5 0.7

Proteins overrepresented in R (fold change, R vs C) Ribosomal proteins (examples) S20, RpsT S21, RpsU S12, RpsL S13, RpsM		 3.0 2.5 2.5 2.3
Proteins overrepresented in C (fold change, C vs R) SstT (sodium: serine/threonine symporter) GrcA (Autonomous glycyl radical cofactor) HutU/HutH (histidine metabolism) KatG (Catalase-peroxidase)	 2.7 2.24 2,0/2,0 1.5	

The center subpopulation contained fewer culturable bacteria, more VBNC cells, and higher levels of CML and AGEs (detected by Western blotting) than the ring subpopulation. Mass spectrometry analyses revealed that the center bacteria contained significantly lower levels of ribosomal proteins. These results were consistent with reports showing that dormant or aging cells lose ribosomes (Bruhn-Olszewska et al., 2018; Helena-Bueno et al., 2024). Other proteome differences included enzymes involved in oxidative stress response (GrcA, KatG), histidine metabolism, and a symporter SstT, which were upregulated in the center.

IV.2.3 *K. pneumoniae* macrocolony cell viability in the center and ring subpopulations

To assess the effect of desiccation on the subpopulations' viability, macrocolonies were incubated at 37 ℃ for up to 13 days. The macrocolonies stopped growing on the 6th day (see **Figure 16**) and their morphology did not change until the end of the experiment (The 13-day macrocolony photos are not available).

In the center subpopulation, the culturable fraction commences modestly at approximately 7% on day 3, signifying limited initial culturability in the center subpopulation, and undergoes a gradual decline to ~5% by day 6, ~1% by day 10, and near 0.1% by day 13, highlighting rapid loss of proliferative capacity under sustained water stress. In parallel, the VBNC subpopulation begins prominently at ~70% on day 3, indicative of swift dormancy induction as a survival tactic, but diminishes progressively to ~35% by day 6, ~25% by day 10, and ~7% by day 13, suggesting VBNC as a fleeting adaptive phase that succumbs to escalating lethality. The dead cell cohort initiates at

~23% on day 3, escalates to ~60% by day 6, ~70% by day 10, and predominates at ~93% by day 13, reflecting cumulative irreversible damage, possibly from oxidative stress and glycation leading to membrane disruption.

In the ring subpopulation, the culturable cell fraction initiates at approximately 30% on day 3, reflecting a substantial fraction of actively culturable cells early in desiccation, then progressively declines to ~9% by day 6, stagnating by day 10, and ~4% by day 13, indicative of escalating loss of culturability as water deprivation intensifies. Concurrently, the VBNC fraction commences high at ~60% on day 3, suggesting rapid entry into dormancy as an adaptive response, with no change by day 6 and mild attenuation to ~50% by day 10, before a sharper drop to ~10% by day 13. This trajectory implies VBNC as a transient refuge, eventually yielding to lethality. The dead cell proportion starts low at ~10% on day 3, surging to ~30% by day 6, then remains relatively stable at ~40% through day 10, and dominates at ~85% by day 13, underscoring cumulative membrane damage, oxidative stress, and irreversible aggregation leading to mortality.

Because the non-mucoid subpopulation evolved from the mucoid center, it was not surprising that, in aging macrocolonies, the ring initially contained more culturable bacteria than the older center subpopulation. However, there was a significant decrease in culturability between days 3 and 6 in the ring (**Figure 18 C**). Furthermore, the rate of loss of viability and the rate at which dead cells appeared during the last 3 days were greater in the ring than in the center (**Figure 18 D**, **E**). The lack of a capsule probably contributed to this effect.

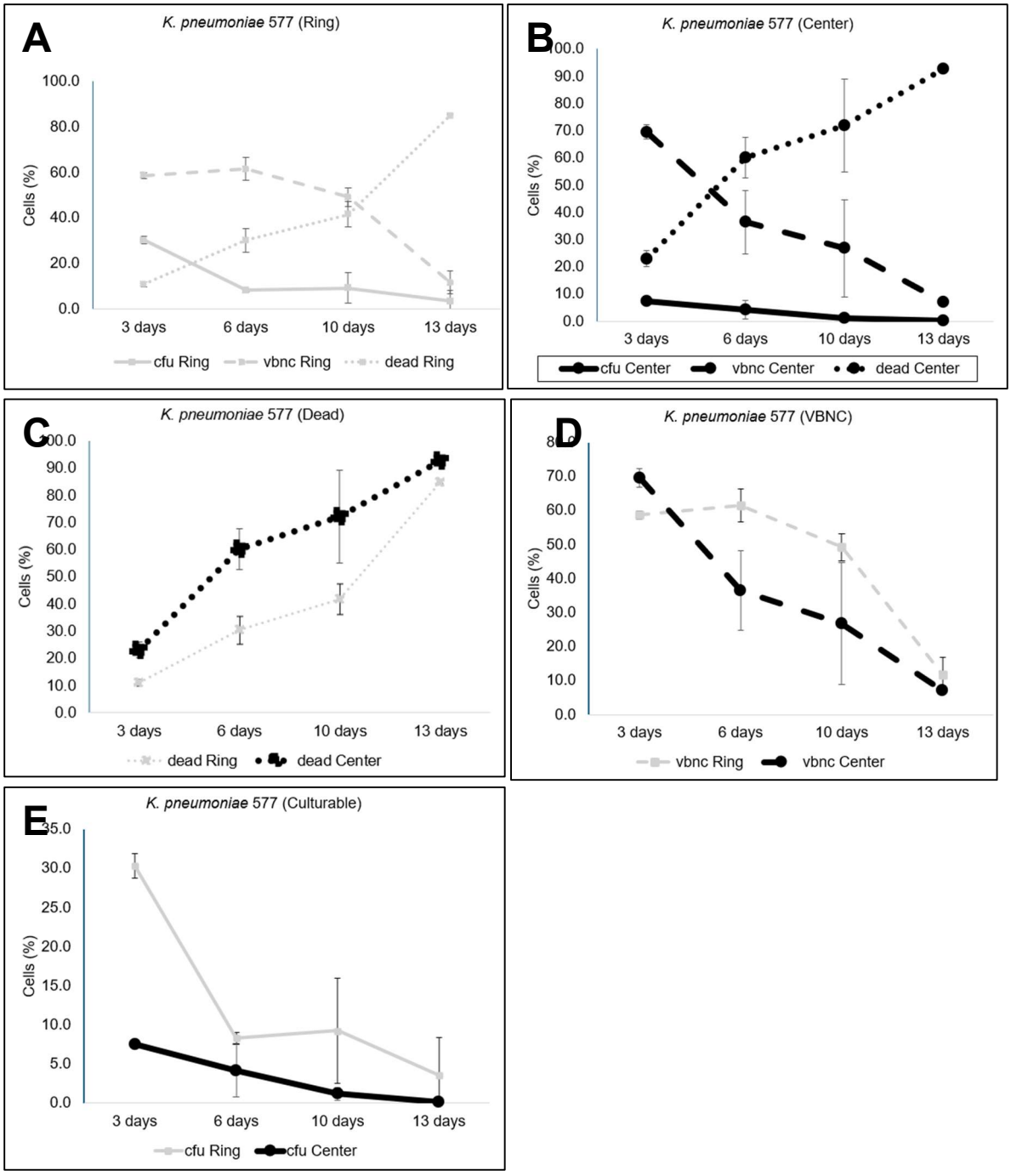

Figure 18. The percentage of culturable, VBNC, and dead cells in the center and ring of *K. pneumoniae* 577-BA. For clarity, the same data were grouped into two sets of graphs: **A** and **B** present the percentages of culturable, VBNC, and dead cells in the center and ring, respectively; panels **C**, **D**, and **F** show the percentages of culturable, VBNC, and dead cells for both subpopulations. Error bars present the standard deviation of three experiments.

IV.2.4 Formation of protein aggregates and glycation products in the center and ring subpopulations

Finally, to test the hypothesis that the extent of protein aggregation is not correlated with bacterial survival, as previous results suggested (**Figure 8**, **Figure 15**), the levels of protein aggregates in the center and ring subpopulations were compared. In this experiment, subpopulations from 6-day macrocolonies, which differ significantly in the percentage of dead cells (~60% in the center vs 30% in the ring, **Figure 18 C**), were used.

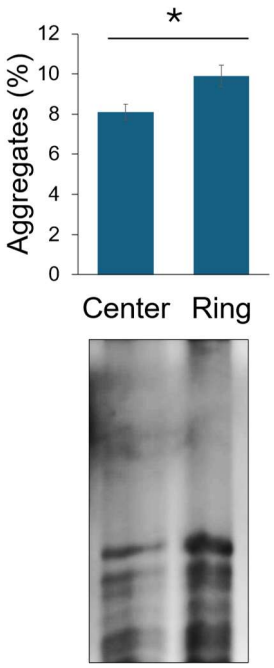

Figure 19. Protein aggregates formation in the center and ring subpopulations isolated from 6-day BA-577 macrocolonies; Error bars represent the standard deviation of three values. A paired two-tailed t-test was used to determine statistical significance (*P < 0.05; **P < 0.01; ***P < 0.001). A representative Coomassie-stained gel is shown

It was found that protein aggregates constitute ~8 and ~10 % of total cell protein isolated from the center and ring subpopulations, respectively (**Figure 19**). Therefore, these results confirmed that, despite higher aggregate levels, the ring subpopulation survives the stress better than the bacteria from the center. As shown in **Table 21**, previous studies demonstrated that the center cells accumulated higher levels of glycation products, namely CML and AGEs (detected by Western blotting), which probably have decreased the viability of this subpopulation.

To better characterize the relationship between *K. pneumoniae* viability and glycation, the change in AGEs levels during macrocolony growth were examined. Additionally, acetyl-lysine levels were also determined, assuming that AGE accumulation may be reduced in cells undergoing protein acetylation as suggested by previous results.

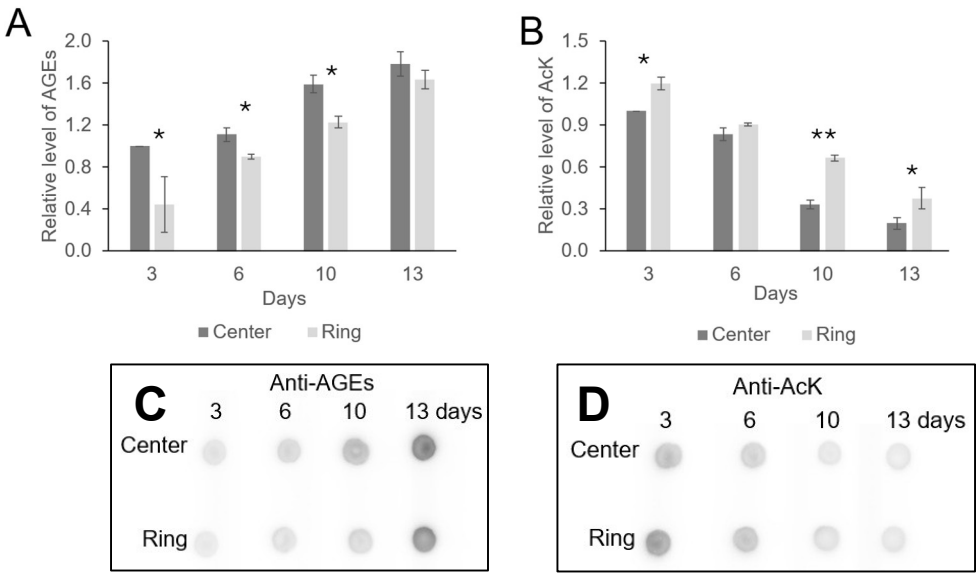

Figure 20. Immunodetection of AGEs and acetyl lysine (AcK) in the center and ring subpopulations collected from 3-, 6-, 10- and 13-day macrocolonies. Whole cell extracts (4 µg of protein) were dot-blotted on a nitrocellulose membrane and analyzed by immunoblotting using and anti-AcK (**A**) and anti-AGEs (**B**) antibodies. The intensity of spots was quantified by densitometry and used to evaluate the level of AGEs and AcK. Representative dot-blots are shown (**C**, **D**). Error bars represent the standard deviation of three values. A paired two-tailed t-test was used to determine statistical significance (*P < 0.05; **P < 0.01; ***P < 0.001). The asterisks represent statistical differences between the center and ring subpopulations.

The initial level of AGEs (3-day macrocolonies) was significantly lower in the ring comparing to the center, but over time the amount of AGEs became comparable in both subpopulations (13-day microcolonies). An opposite effect was observed for AcK—its level was initially higher in the ring, and then constantly decreased in both subpopulations. Therefore, an inverse relationship between glycation and acetylation was observed. It is worth noting that the rate of AGE accumulation in the center and ring was reflected by the rate of loss of viability and cell death in both subpopulations (see **Figure 18**). In 6-day macrocolonies, when a sudden drop in the ring culturability was

observed (**Figure 18 E**), the formation of immunodetected and fluorescent AGEs reached almost the same level in both subpopulations (**Figure 21**).

These results are consistent with observations in *E. coli* (enhanced glycation leading to loss of viability; aggregation-independent survival, **Figure 8**). However, the fluorescence measurements of AGEs at Ex 335 nm/Em 385 nm, Ex 345 nm/Em 404 nm, and Ex 366 nm/Em 442 nm for both ring and center subpopulations maintaining comparable levels (~900–950 a.u.). Overall, these data indicate wavelength-dependent variations in AGE-derived fluorescence, with the center generally showing slightly higher intensities than the ring, except for the pronounced peak in the center at 366/442 nm, potentially reflecting differential glycative stress or metabolic activity across the macrocolony's spatial gradient.

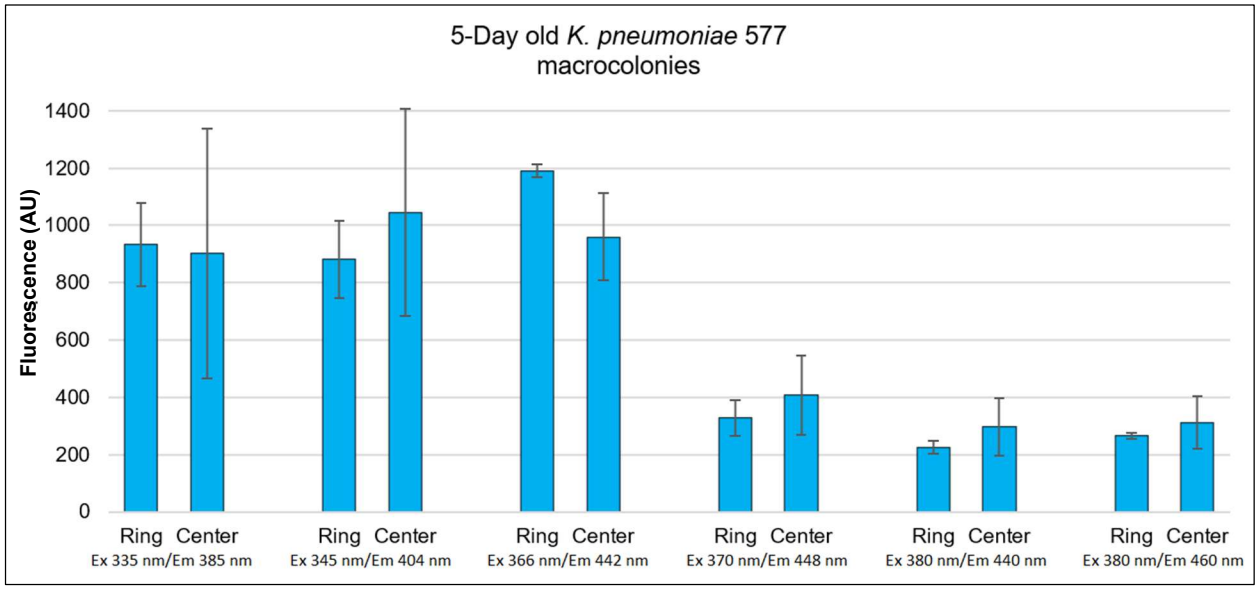

Figure 21. Fluorescent AGE products in two spatially distinct subpopulations (ring vs. center) of 5-day-old *K. pneumoniae* 577-BA macrocolonies grown at 37 ℃.

IV.2.5 Biofilm formation by the center and ring subpopulations

Several studies demonstrated that impaired capsule production affects *in vitro* biofilm formation. Different effects have been observed, depending on the strain and assay conditions. It was found that capsule was required for the adhesion of *K. pneumonia* and biofilm development (Li and Ni, 2023) or, on the contrary, inhibited biofilm formation (Ernst et al., 2020; Nunez et al., 2023). To assess the ability of *K.*

pneumoniae 577-BA to form biofilm, the center and ring cells were resuspended in fresh LB and incubated in polystyrene (PS) or polyvinyl chloride (PVC) microtiter plates at 30 ℃. Overall, biofilm production was weak. However, the absence of the capsule resulted in at least a 2–2.5-fold increase in biofilm mass on both PS and PVC surfaces (**Figure 22**).

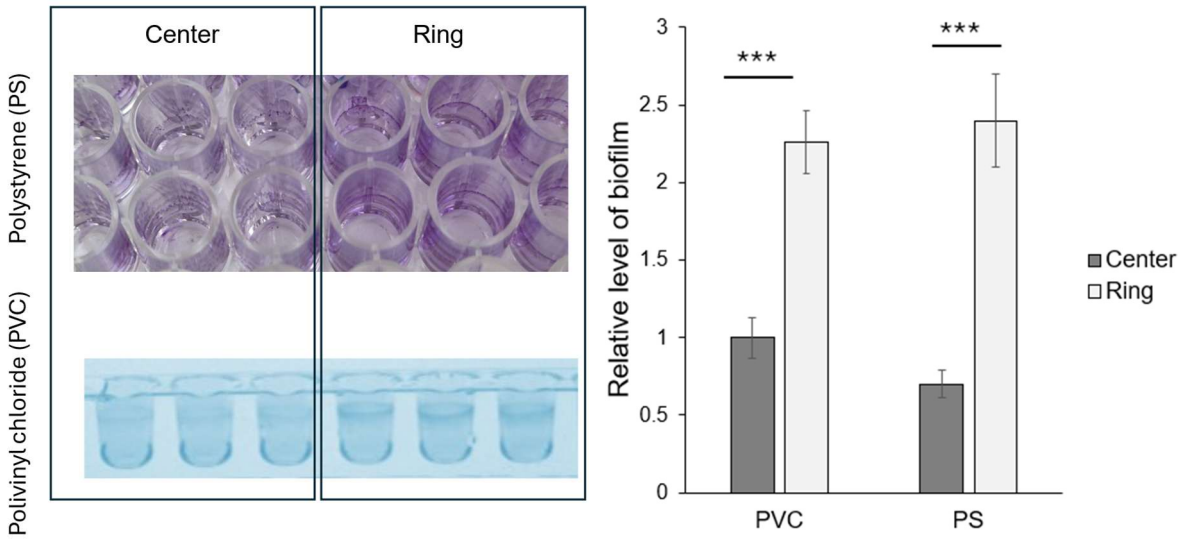

Figure 22. Biofilm formation by the center and ring subpopulations isolated from *K. pneumoniae* macrocolonies. Center and ring cells were resuspended in LB with 0.1 M MOPS pH 7.4 to an $\mathrm{OD}_{595} = 0.01$ and incubated in polystyrene (PS) or polyvinyl chloride (PVC) microtiter plates at 30 ℃ (150 µL per cell) without shaking. After 14 h, bacterial growth was determined by measuring OD_{595}. After removing the planktonic cells from the PVC wells, the biofilm was stained with 0.1% crystal violet for 10 min. After rinsing with water, the attached crystal violet was eluted with a mixture of 80% ethanol and 20% acetone and quantified spectrophotometrically (A_{595}) to calculate the relative amount of biofilm ($\mathrm{A}_{595}/\mathrm{OD}_{595}$). Error bars represent the standard deviation of three values. A paired two-tailed t-test was used to determine statistical significance (*P < 0.05; **P < 0.01; ***P < 0.001).

V3. Comparison of the center and ring subpopulations' genomes

To determine the cause of the ring subpopulation's non-mucoid/non-capsular phenotype, chromosomal DNA isolated from both the ring and center was sequenced on the AVITI NGS platform. Library preparation, sequencing, genome assembly, and a preliminary comparison of the genomes were performed by Genomed (Poland).

Screening of genome assemblies with the Kleborate platform (Galaxy Version 2.3.2+galaxy1) revealed that *K. pneumoniae* 577-BA is an ST329 clone. According to the classification based on K (capsule) antigens and O (lipopolysaccharide, LPS)

antigens, BA-577 belongs to the K27- and O4 serotypes, respectively. The isolate harbores eleven resistant genes to (**Table 22**).

Table 22. Analysis of the center and ring genomes by Kleborate v3 platform (https://usegalaxy.eu/?tool_id=kleborate).

	Center	Ring
Species match	Strong	
Sequence Type	ST392	
***Wzi* allele**	*wzi*187	
Virulence score	0 (negative for all of yersiniabactin, colibactin, aerobactin)	
Resistance score	1 [ESBL, no carbapenemase (regardless of colistin resistance)]	
Number of resistance classes	8	
Number of resistance genes	11	
Resistance genes	Aminoglycoside resistance : aac(6')-Ib-cr.v2;strA.v1^;strB.v1 Fluoroquinolone resistance: qnrB1.v2^ Phenicol resistance: CatB4.v1 Sulfonamide resistance: Sul2 Tetracycline resistance: tet(A).v1 Trimethoprim resistance: dfrA14.v2* Beta lactamases (other than SHV) that have no known extended-spectrum, carbapenemase, or inhibitor-resistance activity: OXA-1;TEM-1D.v1^ Extended-spectrum beta-lactamases, including SHV alleles with known ESBL activity: CTX-M-15 SHV alleles associated with ampicillin resistance only (assumed core chromosomal genes): SHV-11.v1^ Mutations in the SHV beta-lactamase associated with expansion of enzyme activity -35Q Mutations found in the quinolone-resistance determining regions of GyrA and ParC: - GyrA-83I;ParC-80I	
K locus	KL27	
K locus identity	99.28%	
K locus confidence	Very high	Good

	(the locus was found in a single piece with ≥99% coverage and ≥95% identity, with no missing genes and no extra genes).	(the locus was found in a single piece or with ≥95% coverage, with ≤ 3 missing genes and ≤ 1 extra genes)
K locus missing gene		*wbaP*
O locus	O4	
O locus identity	99.71%	
O locus confidence	Very high	

Importantly, the analysis demonstrated that in the ring genome, the *wbaP* gene was missing in the capsule locus. The *wbaP* gene encodes an undecaprenyl-phosphate galactose phosphotransferase that transfers galactose-1-phosphate to undecaprenyl phosphate in the initial step of capsular polysaccharide synthesis (CPS) and the formation of the O-antigen repeating unit of the LPS.

Therefore, the loss of a CPS in the ring subpopulation resulted from the absence of functional WbaP. This result was consistent with other studies showing that insertions or mutations in the *wbaP* gene abolish capsule production (Chiarelli et al., 2020; Ernst et al., 2020; Kaszowska et al., 2021)

Further analysis of the genomes using the Proksee platform (https://proksee.ca; Grant et al., 2023) and IS Finder (https://isfinder.biotoul.fr/) revealed that in the ring chromosome, the *wbaP* gene was disrupted by a mobile element from the Insertion Sequence (IS) 5 family that shows 88% homology to ISKpn74. **Figure 23**–**Figure 24** show a draft map of the BA-577 center reference genome and the CPS locus.

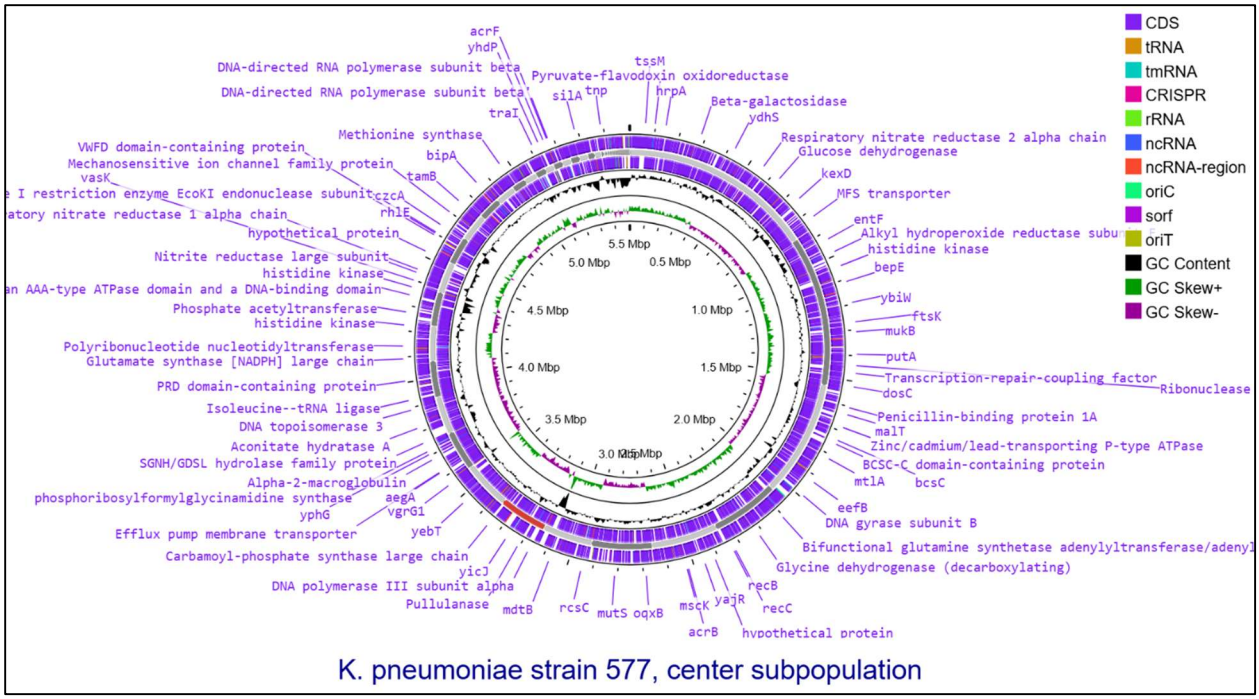

Figure 23. Circular draft genome map per center subpopulation of *K. pneumoniae* 577-BA (5.5 Mb) with concatenated contigs (Nodes) as colored arcs, and GC content as inner black/white plot. The capsule locus with intact wbaP is in Node 8 (magenta arc). The map was generated using Proksee server (https://proksee.ca/).

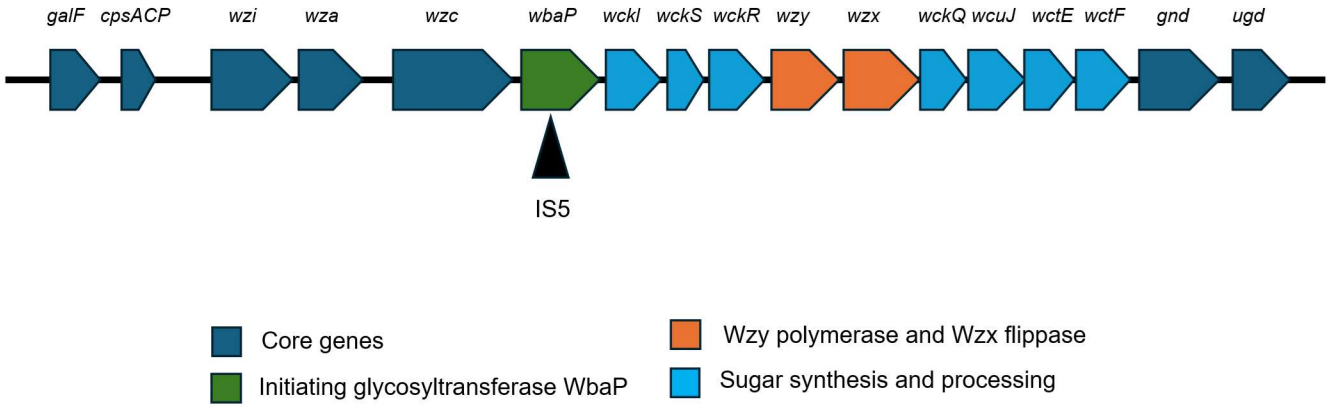

Figure 24. Organization of capsular polysaccharide synthesis (CPS) loci in of *K. pneumoniae* 577-BA. Arrows indicate direction, proportional length, and function of genes (colored as per the legend). The black arrow indicates the insertion of Insertion Sequence (IS)5 in the wbaA gene present in the capsular loci in the ring subpopulation. galF, UTP-glucose-1-phosphate uridylyltransferase; cpsACP, acid phosphatase; wzi, OM protein involved in capsule assembly; wza, polysaccharide export protein; wbaP, undecaprenyl-phosphate galactose phosphotransferase; wckI, glycoside hydrolase; wckS, glycosyltransferase family 2 protein, wckR; glycosyl transferase; wzy, O-antygen polymerase; wzx, flippase; wckQ,galactosyl transferaze; wcuJ, polysaccharide pyruvyl transferase, wctE, glycosyl transferase; wctF, glycosyl transferase; gnd, 6-phosphogluconate dehydrogenase; ugd, UDP-glucose 6-dehydrogenase.

Multiple nonsynonymous SNPs have been detected in the ring genome, but none of the genes with substitutions were directly involved in capsule production (Dorman et al., 2018).

Discussion:

1. Protective protein aggregates in bacteria

Protein misfolding and aggregation may exert multiple detrimental effects in the cell, including loss of function, nonspecific interactions with macromolecules, sequestration of functional proteins, membrane damage, and overload of the protein quality control systems (Bednarska et al., 2013; Mogk et al., 2018). However, increasing evidence indicates that protein aggregates in bacteria play a protective function (Govers et al., 2018; Jin et al., 2021; Wang et al., 2020). Consistent with these studies, the results presented here suggest that protein aggregates exert protective rather than toxic effects, at least during early desiccation-rehydration stress. For example, in the presence of 0.45% betaine or trehalose, *E. coli* cells were partially protected during desiccation, although protein aggregation was significantly increased [**Figure 8 C**]. The next piece of evidence came from the analysis of *K. pneumonia* 577-BA macrocolonies: the more viable ring subpopulation accumulated more aggregates than the less viable center subpopulation (**Figure 19**). In pathogenic bacteria, protein aggregation may lead to dormancy and persistence (Jin et al., 2021; Pu et al., 2019). In accordance with this finding, the ring subpopulation from *K. pneumonia* 577-BA macrocolonies, which accumulated more aggregates (**Figure 19**), produced a higher level of amikacin-persistent cells than the center (Łupkowska, 2025). Further studies are needed to better characterize the protein aggregates and reveal their function in *E. coli* and *K. pneumoniae*. Single-cell experiments using high-resolution microscopy techniques enable the localization of aggregates, the observation of transitions from liquid-like to solid-like states, and their solubilization.

2. Protein glycation in bacteria

Although glycation often results in insoluble cross-linked products (Fournet et al., 2018; Iannuzzi et al., 2014; Rabbani and Thornalley, 2021), the aggregates detected in *E. coli* exposed to desiccation-rehydration stress contain a relatively low level of AGEs. Most glycation products remain soluble (Łupkowska et al., 2023) or, as shown in this work, localize in the outer membrane. The *E. coli* porins OmpC and OmpF were identified with anti-CML antibodies as one of the most glycated proteins (**Figure 7 C**)

Surprisingly, CML was not detected in OmpA, another abundant *E. coli* porin. This may be explained by the fact that lysine glycation depends on the secondary protein structure and the presence of specific glycation hot spots in the vicinity of modified lysines (Bilova et al., 2017; Gazi et al., 2022). OmpC forms trimers of 16-stranded β-barrels, whereas OmpA is a two-domain protein with 8-stranded β-barrel and a globular periplasmatic domain. (Baslé et al., 2006; Samsudin et al., 2016). Out of sixteen lysine residues in OmpC, five are accessible to the solvent and can be modified (Baslé et al., 2006). It can be speculated that neutralization of the positive lysine charge through glycation disrupts the pore's ion selectivity, resulting in loss of culturability and, ultimately, cell death.

Although it is generally believed that protein glycation causes loss of protein function, recent studies have revealed that glycation as a posttranslational modification may regulate the activities of some proteins, including Tle, the type VI secretion system (T6SS) lipase effector from *Enterobacter cloacae* (Jensen et al., 2024). This toxic effector is involved in interbacterial competition and is activated by MGO. The MGO-derived imidazolium cross-link joins the most distant N-terminal and C-terminal helices, thereby stabilizing Tle structure. It is possible that proteins glycated under desiccation-rehydration stress were not trapped in aggregates because cross-links stabilized their native or native-like structure in a soluble form. It is also possible that smaller cross-linked aggregates of non-functional proteins were not separated from the soluble fraction due to limitations of the methods used in this work.

3. Relationship between acetylation and glycation

In vivo and *in vitro* experiments demonstrated that formation of CML may be inhibited by acetylation in *E. coli* (**Figure 10 A, Figure 12 A**). Both glycation and acetylation target lysine residues; therefore, these two modifications may compete with each other under certain conditions. This effect has been reported by multiple studies (Nahomi et al., 2013; Zheng et al., 2019) but has never been observed in bacteria. Since Nε-lysine acetylation neutralizes positively charged lysine side chains and increases hydrophobicity, acetylation may facilitate aggregation. Indeed, acetylation has been found to promote the formation of inclusion bodies and aggregates containing

endogenous *E. coli* proteins (Kuczyńska-Wiśnik et al., 2016; Moruno-Algara et al., 2019). Acetylation is a reversible reaction, whereas CML is stable. Therefore, acetylation could contribute to the formation of protective aggregates that are solubilized after deacetylation upon non-stress conditions. To verify this hypothesis and better understand the interplay between lysine acetylation and glycation in bacteria, further experiments are needed. Specific proteins and lysine residues that are modified by acetylation vs glycation should be identified (in this study, only the bulk overall acetylation/glycation was detected in whole cell extracts or in bacteria (see **Figure 10, Figure 12**). It would be interesting to analyse how acetylation and glycation affect LLPS and the transition of aggregates from liquid- to solid-like state.

4. Protective functions of osmolytes

In *E. coli*, carnosine emerges as the most consistently protective osmolyte across both cellular integrity and protein stability, particularly at a 0.45% concentration, where it modestly reduces protein aggregation after 20 hours of desiccation. This protective effect may stem from its role as a chemical chaperone, safeguarding proteins against desiccation-induced misfolding or aggregation, with enhanced efficacy during rehydration—a phase when proteins are especially vulnerable to denaturation. In contrast, betaine and trehalose exhibit a biphasic response throughout desiccation event: low doses are associated with reduced aggregation, while higher doses promote it, albeit without apparent deleterious consequences, potentially attributable to robust osmotic buffering or protein stabilization during prolonged desiccation.

It remains unclear why osmolytes caused a significant increase in fluorescent AGEs in the *K. pneumonia* MKP103 strain (**Figure 15 A**). *K. pneumonia* MKP103 was much more sensitive to desiccation than *E. coli*. The reason was not different stress conditions (72 hours of drying in a closed Petri dish instead of 4 hours in an open Petri dish). When *E. coli* was incubated under the same conditions as *K. pneumonia* MKP103 there was practically no change in the results.

The exact mechanism by which osmolytes prevent glycation remains unclear. It should be noted that many AGEs are formed through the combination of oxidation and glycation reactions. In addition, glycated residues in proteins are highly reducing and

generate superoxide radicals in the presence of metals. Therefore, osmolyte activities that prevent oxidative stress (Kuczyńska-Wiśnik et al., 2024) may reduce glycation and sustain viability. For example, carnosine acts as a scavenger of metal ions, oxygen radicals, and malondialdehyde (a lipid peroxidation product). It was also found that carnosine directly binds to MGO or carbonyl groups formed during glycation (Hipkiss et al., 2013; Pepper et al., 2010). These multiple protective activities of carnosine inhibited lipid peroxidation (**Figure 6**) maintained membrane integrity and ultimately prevented cell lysis during desiccation-rehydration stress (**Figure 1**). In this study, membrane permeability to PI was used to distinguish between culturable and VBNC bacteria versus dead cells. Fewer PI-positive bacteria, indicating membrane stabilization, were observed in cultures supplemented with all tested osmolytes (**Figure 8 C**). Water substitution and glass transition are other mechanisms through which carnosine and trehalose may prevent protein aggregation (Cao et al., 2022; Laskowska and Kuczyńska-Wiśnik, 2020). It is possible that carnosine, betaine and trehalose serve as chemical chaperones and inhibit the conversion of protective liquid droplets or small aggregates into larger toxic complexes during desiccation-rehydration stress.

5. Macrocolonies of *K. pneumoniae* 577-BA

5.1. *K. pneumoniae* 577-BA genome

K. pneumoniae 577-BA was originally collected through surveillance of groin swabs and was identified as an extended-spectrum beta-lactamase (ESBL)-producing strain. The 577-BA center genome, which was used as a reference sequence, comprises 5,458,465 bp with *5763 genes*.

Analysis of the 577-BA genome with the Kleborate software showed that the isolate belongs to sequence type ST392 and serotypes K27(*wzi187*) and O4. *K. pneumoniae* nosocomial strains were initially mainly limited to ST512, ST258, ST101, and ST307, all of which showed resistance to multiple antibiotics (Tinnirello et al., 2026). Recently, the increasing prevalence of Multidrug-resistant (MDR) ST392 clinical isolates has been observed in various distant locations worldwide (Moreira da Silva et al., 2022). *K. pneumoniae* ST392 clinical or veterinary isolates share a similar resistance profile, including resistance to aminoglycosides, fosfomycin, fluoroquinolones, quinolones, and

sulfonamides (Tinnirello et al., 2026). According to Kleborate, 577-BA shows resistance to all these antibiotic groups except fosfomycin (see **Table 22**). The virulence-associated genes found in the 577-BA genome include OM proteins *ompA* and *tolC*, *fimA* and *fimH* (adhesins, type 2 fimbriae), *pga*ABC and *bcsA*, which are responsible for extracellular polysaccharide production and surface attachment, *entA-F* (enterobactin operon, iron acquisition systems) and *iutA* (aerobactin receptor) involved in iron acquisition. None of the hypervirulence-associated genes encoding yersiniabactin, aerobactin, salmochelin, or colibactin was detected. This is consistent with capsular typing -*the wzi*187 allele was detected, which is not associated with hypervirulent serotypes such as K1 or K2.

5.2 The phenotypic switch from mucoid/capsular to non-mucoid/non-capsular in 577-BA macrocolonies

The phenotypic switch in clinical *K. pneumoniae* isolates from mucoid/capsular to non-mucoid/non-capsular has been observed under laboratory conditions, with heterogeneous colonies appearing on agar plates (Chirelli et al., 2020). Within-host evolution from mucoid to non-mucoid colonies of *K. pneumoniae* isolated from a single patient has also been reported (Lee et al., 2019). In both cases, IS insertions and mutations in genes essential for capsule synthesis caused capsule loss. Similarly, in the 577-BA ring subpopulation, insertion of IS5 into the *wbaP* gene resulted in a non-capsular phenotype. WbaP is a UDP-Gal:phosphoryl-polyprenol Gal-1-phosphate transferase required for the first step in biosynthesis of capsular polysaccharide. WbaP is a member of the polyisoprenyl-phosphate hexose-1-phosphate transferases (PHPT) that catalyze the transfer of hexose-1-P residues from an activated nucleotide diphosphosugar to a lipid carrier. PHPTs initiate biosynthesis of O antigens and capsular polysaccharides, and thereby play an important role in the virulence of various bacteria. Buffet et al. (2021) demonstrated that the maintenance of the capsule depends on the environment: capsule depletion was particularly frequent in nutrient-rich media due to the fitness disadvantage. However, the presence of a capsule increased growth rates and population yields under nutrient-poor conditions. Kaszowska et al. (2021) found that *wbaP* inactivation and capsule loss led to overproduction of LPS but did not affect bacterial fitness or the insensitivity to serum complement. However, bacteria lacking a

capsule were more prone to phagocytosis and internalization by human lung epithelial cells. Other studies showed that loss of capsule production in different *K. pneumoniae* led to increased or decreased, depending on the strain, susceptibility to carbapenems, biofilm formation and autoaggregation (Chirelli et al., 2020). Subpopulations that differ in susceptibility to meropenem and in their ability to form biofilm were also observed in macrocolonies of the New Delhi metallo-β-lactamase (NDM)-1-producing *Enterobacter hormaeche* clinical isolate (Brust et al. 2019).

As mentioned above, 577-BA lacks hypervirulence-associated genes, but the presence of two subpopulations, capsulated and non-capsulated, may enable the strain to better adapt to changing environmental conditions and likely evade the host immune response. The ring subpopulation contained slightly more aggregates than the center (**Figure 19**). Whether they serve a protective function and whether they confer an advantage remains to be determined. First, it would be necessary to identify the aggregate components and determine whether they undergo glycation or acetylation. The proteins visible on the gel have low molecular weights, which may suggest that they are predominantly ribosomal proteins. 577-BA did not develop a robust biofilm; nevertheless, loss of the capsule in the ring subpopulation significantly increased biofilm formation on plastic surfaces by at least 2-fold, probably due to enhanced hydrophobicity of non-capsulated cells (**Figure 22**, **Table 23**). The conditions in the center favored heteroresistance to colistin, e.g., the emergence of sub-subpopulations with high-level resistance to colistin, whereas the ring produced more persisters—dormant bacteria, phenotypic variants of WT cell, that can withstand antibiotic treatment. All studies in this section suggest that new phenotypes arising from capsule loss could significantly impede diagnosis and antibiotic treatment.

Table 23. Biofilm formation capacity, antibiotic heteroresistance or persistence

	Center (mucoid)	Ring (non-mucoid)	Reference
Relative biofilm mass	1	~2.3-2.5	This work
Heteroresistance to colistin (100% -total cell number in the subpopulation)	0.003 %	0.0003%	(Łupkowska, 2025)
Persistence to amikacin Persistence to meropenem (100% -total cell number in the subpopulation)	0.14% 0.12 %	0.26% 0.15%	(Łupkowska, 2025)
Protective aggregates? (100% -whole cell extract protein)	~8%	~10%	This work

The results presented in this dissertation provide new insights into protein aggregation, glycation, and the role of osmolytes in protecting bacteria from desiccation-rehydration stress. The main conclusion is that glycation, rather than protein aggregation, is the primary cause of bacterial death, whereas aggregates may fulfill protective functions during desiccation-rehydration stress. Since protein aggregation is a strategy used by pathogens to survive antibiotic treatment, the results presented may serve as a basis for future studies aimed at developing successful antibacterial therapies.

Conclusion

It was found that lower concentrations of carnosine, betaine, and trehalose inhibited the formation of protein aggregates and glycation products, resulting in increased *E. coli* viability under desiccation-rehydration stress. Although high concentrations of betaine and trehalose significantly enhanced protein aggregation, glycation was still inhibited and *E. coli* cells survived desiccation better than bacteria grown without osmolytes. These results suggest that 1) glycation rather than protein aggregation is the main cause of *E. coli* death upon desiccation-rehydration stress, 2) the aggregates may fulfill protective functions during early desiccation-rehydration stress.

In vitro and *in vivo* experiments showed that Nε-lysine acetylation may prevent the formation of CML, one of the non-fluorescent AGEs in *E. coli.*

Regardless of the concentration used, the osmolytes significantly enhanced protein aggregation in *K. pneumoniae* MKP103 and moderately improved viability under desiccation-rehydration stress. It remains unclear why osmolytes simultaneously inhibited the formation of immunodetected AGEs and enhanced the accumulation of fluorescent AGEs.

The appearance of the non-mucoid/noncapsular ring subpopulation *in K. pneumoniae* 577-BA macrocolonies resulted from IS5 insertion into the *wbaP* gene, which encodes undecaprenyl-phosphate galactose phosphotransferase, an enzyme catalyzing the first step of capsule production. The lack of capsule facilitated biofilm formation by the ring subpopulation.

Despite higher protein aggregation, the ring subpopulation showed increased viability and reduced initial AGE accumulation compared with the mucoid/capsular center subpopulation.

Taken together, these results suggest that, similar to *E. coli*, glycation rather than the accumulation of aggregated proteins may be the cause of loss of viability in *K. pneumoniae*.

Bibliography

Baslé, Arnaud, Gabriele Rummel, Paola Storici, Juerg P. Rosenbusch, and Tilman Schirmer. "Crystal structure of osmoporin OmpC from E. coli at 2.0 Å." *Journal of molecular biology* 362, no. 5 (2006): 933-942.

Bednarska, Natalia G., Joost Schymkowitz, Frederic Rousseau, and Johan Van Eldere. "Protein aggregation in bacteria: the thin boundary between functionality and toxicity." *Microbiology* 159, no. Pt_9 (2013): 1795-1806.

Bilova, Tatiana, Gagan Paudel, Nikita Shilyaev, Rico Schmidt, Dominic Brauch, Elena Tarakhovskaya, Svetlana Milrud et al. "Global proteomic analysis of advanced glycation end products in the Arabidopsis proteome provides evidence for age-related glycation hot spots." *Journal of Biological Chemistry* 292, no. 38 (2017): 15758-15776.

Boldyrev, Alexander A., Giancarlo Aldini, and Wim Derave. "Physiology and pathophysiology of carnosine." *Physiological reviews* (2013).

Bollen, Celien, Sofie Louwagie, Femke Deroover, Wouter Duverger, Ladan Khodaparast, Laleh Khodaparast, Dieter Hofkens et al. "Composition and liquid-to-solid maturation of protein aggregates contribute to bacterial dormancy development and recovery." *Nature Communications* 16, no. 1 (2025): 1046.

Borzova, Vera A., Svetlana G. Roman, Anastasiya V. Pivovarova, and Natalia A. Chebotareva. "Effects of molecular crowding and betaine on HSPB5 interactions, with target proteins differing in the quaternary structure and aggregation mechanism." *International Journal of Molecular Sciences* 23, no. 23 (2022): 15392.

Boteva, Elitsa, and Roumyana Mironova. "Maillard reaction and aging: can bacteria shed light on the link?." *Biotechnology & Biotechnological Equipment* 33, no. 1 (2019): 481-497.

Brauer, Adrienne M., Handuo Shi, Petra Anne Levin, and Kerwyn Casey Huang. "Physiological and regulatory convergence between osmotic and nutrient stress responses in microbes." *Current Opinion in Cell Biology* 81 (2023): 102170.

Bruhn-Olszewska, Bożena, Paweł Szczepaniak, Ewelina Matuszewska, Dorota Kuczyńska-Wiśnik, Karolina Stojowska-Swędrzyńska, María Moruno Algara, and Ewa Laskowska. "Physiologically distinct subpopulations formed in Escherichia coli cultures in response to heat shock." *Microbiological research* 209 (2018): 33-42.

Brust, Flávia Roberta, Luana Boff, Danielle da Silva Trentin, Franciele Pedrotti Rozales, Afonso Luís Barth, and Alexandre José Macedo. "Macrocolony of NDM-1 producing Enterobacter hormaechei subsp. oharae generates subpopulations with different features regarding the response of antimicrobial agents and biofilm formation." *Pathogens* 8, no. 2 (2019): 49.

Buffet, Amandine, Eduardo PC Rocha, and Olaya Rendueles. "Nutrient conditions are primary drivers of bacterial capsule maintenance in Klebsiella." *Proceedings of the Royal Society B* 288, no. 1946 (2021): 20202876.

Burg, Maurice B., and Joan D. Ferraris. "Intracellular organic osmolytes: function and regulation." *Journal of Biological Chemistry* 283, no. 12 (2008): 7309-7313.

Burgess, Patrick, and Bingru Huang. "Mechanisms of hormone regulation for drought tolerance in plants." In Drought Stress Tolerance in Plants, Vol 1: Physiology and Biochemistry, pp. 45-75. Cham: Springer International Publishing, 2016.

Cao, Ruodan, Tomochika Sogabe, Shuto Mikajiri, and Kiyoshi Kawai. "Effects of sucrose, carnosine, and their mixture on the glass transition behavior and storage stability of freeze-dried lactic acid bacteria at various water activities." *Cryobiology* 106 (2022): 131-138.

Caruso, Giuseppe, Lucia Di Pietro, Vincenzo Cardaci, Salvatore Maugeri, and Filippo Caraci. "The therapeutic potential of carnosine: Focus on cellular and molecular mechanisms." *Current Research in Pharmacology and Drug Discovery* 4 (2023): 100153.

Caruso, Giuseppe. "Unveiling the hidden therapeutic potential of carnosine, a molecule with a multimodal mechanism of action: a position paper." *Molecules* 27, no. 10 (2022): 3303.

Cayley, Scott, and M. Thomas Record. "Roles of cytoplasmic osmolytes, water, and crowding in the response of Escherichia coli to osmotic stress: biophysical basis of osmoprotection by glycine betaine." *Biochemistry* 42, no. 43 (2003): 12596-12609.

Chen, Xiao, Kefan Fang, Bo Li, Yingxing Li, Yuehua Ke, Weixin Ke, Tian Tian et al. "Macrophage-derived reactive oxygen species promote Salmonella aggresome formation contributing to bacterial antibiotic persistence." *iMeta* (2025): e70059.

Chiarelli, Adriana, Nicolas Cabanel, Isabelle Rosinski-Chupin, Pengdbamba Dieudonné Zongo, Thierry Naas, Rémy A. Bonnin, and Philippe Glaser. "Diversity of mucoid to non-mucoid switch among carbapenemase-producing Klebsiella pneumoniae." *BMC microbiology* 20, no. 1 (2020): 325.

Chmielewska, Klaudia, Krystyna Dzierzbicka, Iwona Inkielewicz-Stepniak, and Maja Przybyłowska. "Therapeutic potential of carnosine and its derivatives in the treatment of human diseases." *Chemical Research in Toxicology* 33, no. 7 (2020): 1561-1578.

Cohen-Or, Ifat, Chen Katz, and Eliora Z. Ron. "AGEs secreted by bacteria are involved in the inflammatory response." *PLoS One* 6, no. 3 (2011): e17974.

Cohen-Or, Ifat, Chen Katz, and Eliora Z. Ron. "Metabolism of AGEs–Bacterial AGEs are degraded by metallo-proteases." *PLoS One* 8, no. 10 (2013): e74970.

Conlan, Sean, Morgan Park, Clayton Deming, Pamela J. Thomas, Alice C. Young, Holly Coleman, Christina Sison et al. "Plasmid dynamics in KPC-positive Klebsiella pneumoniae during long-term patient colonization." *MBio* 7, no. 3 (2016): 10-1128.

Conlan, Sean, Pamela J. Thomas, Clayton Deming, Morgan Park, Anna F. Lau, John P. Dekker, Evan S. Snitkin et al. "Single-molecule sequencing to track plasmid diversity

of hospital-associated carbapenemase-producing Enterobacteriaceae." *Science translational medicine* 6, no. 254 (2014): 254ra126-254ra126.

Dorman, Matthew J., Theresa Feltwell, David A. Goulding, Julian Parkhill, and Francesca L. Short. "The capsule regulatory network of Klebsiella pneumoniae defined by density-TraDISort." *MBio* 9, no. 6 (2018): 10-1128.

Ernst, Christoph M., Julian R. Braxton, Carlos A. Rodriguez-Osorio, Anna P. Zagieboylo, Li Li, Alejandro Pironti, Abigail L. Manson et al. "Adaptive evolution of virulence and persistence in carbapenem-resistant Klebsiella pneumoniae." *Nature medicine* 26, no. 5 (2020): 705-711.

Fournet, Maxime, Frédéric Bonté, and Alexis Desmoulière. "Glycation damage: a possible hub for major pathophysiological disorders and aging." *Aging and disease* 9, no. 5 (2018): 880.

Fu, Min-Xin, Jesus R. Requena, Alicia J. Jenkins, Timothy J. Lyons, John W. Baynes, and Suzanne R. Thorpe. "The Advanced glycation end product, N∈-(Carboxymethyl) lysine, is a product of both lipid peroxidation and glycoxidation reactions (∗)." *Journal of Biological Chemistry* 271, no. 17 (1996): 9982-9986.

Gazi, Inge, Vojtech Franc, Sem Tamara, Martine P. van Gool, Thom Huppertz, and Albert JR Heck. "Identifying glycation hot-spots in bovine milk proteins during production and storage of skim milk powder." *International Dairy Journal* 129 (2022): 105340.

Govers, Sander K., Julien Mortier, Antoine Adam, and Abram Aertsen. "Protein aggregates encode epigenetic memory of stressful encounters in individual Escherichia coli cells." *PLoS biology* 16, no. 8 (2018): e2003853.

Grant, Jason R., Eric Enns, Eric Marinier, Arnab Mandal, Emily K. Herman, Chih-yu Chen, Morag Graham, Gary Van Domselaar, and Paul Stothard. "Proksee: in-depth characterization and visualization of bacterial genomes." *Nucleic acids research* 51, no. W1 (2023): W484-W492.

Gupta, Saurabh, Sangam Jha, Chiranjit Mahato, and Dibyendu Das. "Non-equilibrium demixing and dissolution of chiral coacervates via intrinsic catalysis." Nature Communications 16, no. 1 (2025): 9336.

Helena-Bueno, Karla, Lewis I. Chan, and Sergey V. Melnikov. "Rippling life on a dormant planet: hibernation of ribosomes, RNA polymerases, and other essential enzymes." *Frontiers in Microbiology* 15 (2024): 1386179.

Hipkiss, Alan R., Stephanie P. Cartwright, Clare Bromley, Stephane R. Gross, and Roslyn M. Bill. "Carnosine: can understanding its actions on energy metabolism and protein homeostasis inform its therapeutic potential?." Chemistry Central Journal 7, no. 1 (2013): 38.

Iannuzzi, Clara, Gaetano Irace, and Ivana Sirangelo. "Differential effects of glycation on protein aggregation and amyloid formation." *Frontiers in molecular biosciences* 1 (2014): 9.

Jensen, Steven J., Bonnie J. Cuthbert, Fernando Garza-Sánchez, Colette C. Helou, Rodger de Miranda, Celia W. Goulding, and Christopher S. Hayes. "Advanced glycation end-product crosslinking activates a type VI secretion system phospholipase effector protein." *Nature communications* 15, no. 1 (2024): 8804.

Jin, X., J. E. Lee, C. Schaefer, X. Luo, A. J. M. Wollman, A. L. Payne-Dwyer, T. Tian, X. Zhang, X. Chen, and Y. Li. *Membraneless organelles formed by liquid-liquid phase separation increase bacterial fitness. Sci Adv. 2021: 7 (43): eabh2929*.

Jukić, Ivana, Nikolina Kolobarić, Ana Stupin, Anita Matić, Nataša Kozina, Zrinka Mihaljević, Martina Mihalj et al. "Carnosine, small but mighty—prospect of use as functional ingredient for functional food formulation." *Antioxidants* 10, no. 7 (2021): 1037.

Jung, Kirsten, Knut Hamann, and Anne Revermann. "K+ stimulates specifically the autokinase activity of purified and reconstituted EnvZ of Escherichia coli." *Journal of Biological Chemistry* 276, no. 44 (2001): 40896-40902.

Kaszowska, Marta, Grazyna Majkowska-Skrobek, Pawel Markwitz, Cédric Lood, Wojciech Jachymek, Anna Maciejewska, Jolanta Lukasiewicz, and Zuzanna Drulis-Kawa. "The mutation in wbaP cps gene cluster selected by phage-borne depolymerase abolishes capsule production and diminishes the virulence of Klebsiella pneumoniae." *International journal of molecular sciences* 22, no. 21 (2021): 11562.

Kaushik, Jai K., and Rajiv Bhat. "Why Is Trehalose an Exceptional Protein Stabilizer?: An analysis of the thermal stability of proteins in the presence of the compatible osmolyte trehalose." *Journal of Biological Chemistry* 278, no. 29 (2003): 26458-26465.

Khalifeh, Masoomeh, George E. Barreto, and Amirhossein Sahebkar. "Trehalose as a promising therapeutic candidate for the treatment of Parkinson's disease." *British journal of pharmacology* 176, no. 9 (2019): 1173-1189.

Khan, Sobia, Seerat Siraj, Mohammad Shahid, Mohammad Mahfuzul Haque, and Asimul Islam. "Osmolytes: Wonder molecules to combat protein misfolding against stress conditions." *Int J Biol Macromol* 234, no. 123662 (2023): 10-1016.

Kim, Jessica Y., and Norbert W. Seidler. "Carnosine promotes GAPDH dimer formation: proposed role in preventing neurodegeneration." (2011): 572-6.

Kram, Karin E., and Steven E. Finkel. "Culture volume and vessel affect long-term survival, mutation frequency, and oxidative stress of Escherichia coli." *Applied and environmental microbiology* 80, no. 5 (2014): 1732-1738.

Kram, Karin E., and Steven E. Finkel. "Rich medium composition affects Escherichia coli survival, glycation, and mutation frequency during long-term batch culture." *Applied and environmental microbiology* 81, no. 13 (2015): 4442-4450.

Książek, Krzysztof. "Bacterial aging: from mechanistic basis to evolutionary perspective." *Cellular and molecular life sciences* 67, no. 18 (2010): 3131-3137.

Kuczyńska-Wiśnik, Dorota, Karolina Stojowska-Swędrzyńska, and Ewa Laskowska. "Intracellular protective functions and therapeutical potential of trehalose." *Molecules* 29, no. 9 (2024): 2088.

Kuczyńska-Wiśnik, Dorota, Karolina Stojowska-Swędrzyńska, and Ewa Laskowska. "Liquid–Liquid Phase Separation and protective protein aggregates in bacteria." *Molecules* 28, no. 18 (2023): 6582.

Kuczyńska-Wiśnik, Dorota, María Moruno-Algara, Karolina Stojowska-Swędrzyńska, and Ewa Laskowska. "The effect of protein acetylation on the formation and processing of inclusion bodies and endogenous protein aggregates in Escherichia coli cells." *Microbial Cell Factories* 15, no. 1 (2016): 189.

Kushwah, Neetu, Vishal Jain, and Dhananjay Yadav. "Osmolytes: A possible therapeutic molecule for ameliorating the neurodegeneration caused by protein misfolding and aggregation." *Biomolecules* 10, no. 1 (2020): 132.

Kuzan, Aleksandra. "Toxicity of advanced glycation end products." *Biomedical Reports* 14, no. 5 (2021): 46.

Laskowska, Ewa, and Dorota Kuczyńska-Wiśnik. "New insight into the mechanisms protecting bacteria during desiccation." *Current genetics* 66, no. 2 (2020): 313-318.

Lee, Haejeong, Juyoun Shin, Yeun-Jun Chung, Jin Yang Baek, Doo Ryeon Chung, Kyong Ran Peck, Jae-Hoon Song, and Kwan Soo Ko. "Evolution of Klebsiella pneumoniae with mucoid and non-mucoid type colonies within a single patient." *International Journal of Medical Microbiology* 309, no. 3-4 (2019): 194-198.

Leibly, David J., Trang Nhu Nguyen, Louis T. Kao, Stephen N. Hewitt, Lynn K. Barrett, and Wesley C. Van Voorhis. "Stabilizing additives added during cell lysis aid in the solubilization of recombinant proteins." *PloS one* 7, no. 12 (2012): e52482.

Leiva-Sabadini, Camila, Pablo Berríos, Paula Saavedra, Javiera Carrasco-Rojas, José Vicente González-Aramundiz, Mario Vera, Estefanía Tarifeño-Saldivia, Christina MAP Schuh, and Sebastian Aguayo. "Biofilm formation on glycated collagen modulates Streptococcus mutans bacterial extracellular vesicle production and cargo." *bioRxiv* (2024): 2024-12.

Leszczynska, Daria, Ewelina Matuszewska, Dorota Kuczynska-Wisnik, Beata Furmanek-Blaszk, and Ewa Laskowska. "The formation of persister cells in stationary-phase cultures of Escherichia coli is associated with the aggregation of endogenous proteins." *PLoS One* 8, no. 1 (2013): e54737.

Li, Yin, and Ming Ni. "Regulation of biofilm formation in Klebsiella pneumoniae." *Frontiers in microbiology* 14 (2023): 1238482.

Lindner, Ariel B., Richard Madden, Alice Demarez, Eric J. Stewart, and François Taddei. "Asymmetric segregation of protein aggregates is associated with cellular aging and rejuvenation." *Proceedings of the National Academy of Sciences* 105, no. 8 (2008): 3076-3081.

Łupkowska, Adrianna, Soroosh Monem, Janusz Dębski, Karolina Stojowska-Swędrzyńska, Dorota Kuczyńska-Wiśnik, and Ewa Laskowska. "Protein aggregation and glycation in Escherichia coli exposed to desiccation-rehydration stress." *Microbiological Research* 270 (2023): 127335.

Łupkowska, Adrianna. "Escherichia coli and Klebsiella pneumoniae Persisters Formed under Stressful Conditions." PhD diss., University of Gdańsk, 2025.

Matuszewska, Ewelina, Joanna Kwiatkowska, Dorota Kuczyńska-Wiśnik, and Ewa Laskowska. "Escherichia coli heat-shock proteins IbpA/B are involved in resistance to oxidative stress induced by copper." *Microbiology* 154, no. 6 (2008): 1739-1747.

May, Gerhard, Elke Faatz, Merna Villarejo, and Erhard Bremer. "Binding protein dependent transport of glycine betaine and its osmotic regulation in Escherichia coli K12." *Molecular and General Genetics MGG* 205, no. 2 (1986): 225-233.

Miotto, Mattia, Nina Warner, Giancarlo Ruocco, Gian Gaetano Tartaglia, Oren A. Scherman, and Edoardo Milanetti. "Osmolyte-induced protein stability changes explained by graph theory." *Computational and Structural Biotechnology Journal* 23 (2024): 4077-4087.

Mironova, Roumyana, Toshimitsu Niwa, Hideki Hayashi, Rositsa Dimitrova, and Ivan Ivanov. "Evidence for non-enzymatic glycosylation in Escherichia coli." *Molecular microbiology* 39, no. 4 (2001): 1061-1068.

Mironova, Roumyana, Toshimitsu Niwa, Yordan Handzhiyski, Angelina Sredovska, and Ivan Ivanov. "Evidence for non-enzymatic glycosylation of Escherichia coli chromosomal DNA." *Molecular microbiology* 55, no. 6 (2005): 1801-1811.

Mogk, Axel, Bernd Bukau, and Harm H. Kampinga. "Cellular handling of protein aggregates by disaggregation machines." *Molecular cell* 69, no. 2 (2018): 214-226.

Morbach, Susanne, and Reinhard Krämer. "Osmoregulation and osmosensing by uptake carriers for compatible solutes in bacteria." In *Molecular Mechanisms Controlling Transmembrane Transport*, pp. 121-153. Berlin, Heidelberg: Springer Berlin Heidelberg, 2004.

Moreira da Silva, Joana, Juliana Menezes, Gabriel Mendes, Sofia Santos Costa, Cátia Caneiras, Laurent Poirel, Andreia J. Amaral, and Constança Pomba. "KPC-3-producing Klebsiella pneumoniae sequence type 392 from a dog's clinical isolate in Portugal." *Microbiology spectrum* 10, no. 4 (2022): e00893-22.

Moruno Algara, María, Dorota Kuczyńska-Wiśnik, Janusz Dębski, Karolina Stojowska-Swędrzyńska, Hanna Sominka, Małgorzata Bukrejewska, and Ewa Laskowska. "Trehalose protects Escherichia coli against carbon stress manifested by protein acetylation and aggregation." *Molecular Microbiology* 112, no. 3 (2019): 866-880.

Mukherjee, Mrinmoy, and Jagannath Mondal. "Heterogeneous impacts of protein-stabilizing osmolytes on hydrophobic interaction." *The Journal of Physical Chemistry B* 122, no. 27 (2018): 6922-6930.

Nahomi, Rooban B., Tomoko Oya-Ito, and Ram H. Nagaraj. "The combined effect of acetylation and glycation on the chaperone and anti-apoptotic functions of human α-crystallin." *Biochimica et Biophysica Acta (BBA)-Molecular Basis of Disease* 1832, no. 1 (2013): 195-203.

Natalello, Antonino, Jing Liu, Diletta Ami, Silvia Maria Doglia, and Ario de Marco. "The osmolyte betaine promotes protein misfolding and disruption of protein aggregates." *Proteins: Structure, Function, and Bioinformatics* 75, no. 2 (2009): 509-517.

Nunez, Charles, Xenia Kostoulias, Anton Y. Peleg, Francesca Short, and Yue Qu. "A comprehensive comparison of biofilm formation and capsule production for bacterial survival on hospital surfaces." *Biofilm* 5 (2023): 100105.

Orban, Katie, and Steven E. Finkel. "Dps is a universally conserved dual-action DNA-binding and ferritin protein." *Journal of Bacteriology* 204, no. 5 (2022): e00036-22.

Patel, Kinjal A., Ratnika Sethi, Anita R. Dhara, and Ipsita Roy. "Challenges with osmolytes as inhibitors of protein aggregation: Can nucleic acid aptamers provide an answer?." *International journal of biological macromolecules* 100 (2017): 75-88.

Pei, Linsen, Yujia Xian, Xiaodan Yan, Charley Schaefer, Aisha H. Syeda, Jamieson AL Howard, Wei Zhang et al. "Aggresomes protect mRNA under stress in Escherichia coli." *Nature Microbiology* 10, no. 9 (2025): 2323-2337.

Pepelnjak, Monika, Britta Velten, Nicolas Näpflin, Tatjana von Rosen, Umberto Capasso Palmiero, Jeong Hoon Ko, Heather D. Maynard et al. "In situ analysis of osmolyte mechanisms of proteome thermal stabilization." *Nature Chemical Biology* 20, no. 8 (2024): 1053-1065.

Pepper, Evan D., Michael J. Farrell, Gary Nord, and Steven E. Finkel. "Antiglycation effects of carnosine and other compounds on the long-term survival of Escherichia coli." *Applied and environmental microbiology* 76, no. 24 (2010): 7925-7930.

Perrone, Anna, Antonio Giovino, Jubina Benny, and Federico Martinelli. "Advanced glycation end products (AGEs): biochemistry, signaling, analytical methods, and epigenetic effects." *Oxidative medicine and cellular longevity* 2020, no. 1 (2020): 3818196.

Perroud, Bertrand, and Daniel Le Rudulier. "Glycine betaine transport in Escherichia coli: osmotic modulation." *Journal of bacteriology* 161, no. 1 (1985): 393-401.

Plotkin, Balbina J., Scott Halkyard, Emily Spoolstra, Amanda Micklo, Amber Kaminski, Ira M. Sigar, and Monika I. Konaklieva. "The role of the insulin/glucose ratio in the regulation of pathogen biofilm formation." *Biology* 12, no. 11 (2023): 1432.

Potts, Malcolm, Stephen M. Slaughter, Frank-U. Hunneke, James F. Garst, and Richard F. Helm. "Desiccation tolerance of prokaryotes: application of principles to human cells." *Integrative and Comparative Biology* 45, no. 5 (2005): 800-809.

Pu, Yingying, Yingxing Li, Xin Jin, Tian Tian, Qi Ma, Ziyi Zhao, Ssu-yuan Lin et al. "ATP-dependent dynamic protein aggregation regulates bacterial dormancy depth critical for antibiotic tolerance." *Molecular cell* 73, no. 1 (2019): 143-156.

Rabbani, Naila, Mingzhan Xue, and Paul J. Thornalley. "Dicarbonyl stress, protein glycation and the unfolded protein response." *Glycoconjugate Journal* 38, no. 3 (2021): 331-340.

Ravitchandirane, Gayathri, Sheetal Bandhu, and Tapan K. Chaudhuri. "Multimodal approaches for the improvement of the cellular folding of a recombinant iron regulatory protein in E. coli." *Microbial Cell Factories* 21, no. 1 (2022): 20.

Rokney, Assaf, Merav Shagan, Martin Kessel, Yoav Smith, Ilan Rosenshine, and Amos B. Oppenheim. "E. coli transports aggregated proteins to the poles by a specific and energy-dependent process." *Journal of molecular biology* 392, no. 3 (2009): 589-601.

Ruhal, Rohit, Rashmi Kataria, and Bijan Choudhury. "Trends in bacterial trehalose metabolism and significant nodes of metabolic pathway in the direction of trehalose accumulation." *Microbial Biotechnology* 6, no. 5 (2013): 493-502.

Rungratanawanich, Wiramon, Ying Qu, Xin Wang, Musthafa Mohamed Essa, and Byoung-Joon Song. "Advanced glycation end products (AGEs) and other adducts in aging-related diseases and alcohol-mediated tissue injury." *Experimental & molecular medicine* 53, no. 2 (2021): 168-188.

Samsudin, Firdaus, Maite L. Ortiz-Suarez, Thomas J. Piggot, Peter J. Bond, and Syma Khalid. "OmpA: a flexible clamp for bacterial cell wall attachment." *Structure* 24, no. 12 (2016): 2227-2235.

Séro, Luc, Lionel Sanguinet, Patricia Blanchard, Bach Tai Dang, Sylvie Morel, Pascal Richomme, Denis Séraphin, and Séverine Derbré. "Tuning a 96-well microtiter plate fluorescence-based assay to identify AGE inhibitors in crude plant extracts." *Molecules* 18, no. 11 (2013): 14320-14339.

Shek, Yuen Lai, and Tigran V. Chalikian. "Interactions of glycine betaine with proteins: insights from volume and compressibility measurements." *Biochemistry* 52, no. 4 (2013): 672-680.

Singh, Laishram R., Tanveer Ali Dar, Safikur Rahman, Shazia Jamal, and Faizan Ahmad. "Glycine betaine may have opposite effects on protein stability at high and low pH values." *Biochimica et Biophysica Acta (BBA)-Proteins and Proteomics* 1794, no. 6 (2009): 929-935.

Sleator, Roy D., and Colin Hill. "Bacterial osmoadaptation: the role of osmolytes in bacterial stress and virulence." *FEMS microbiology reviews* 26, no. 1 (2002): 49-71.

Sleutel, Mike, Imke Van den Broeck, Nani Van Gerven, Cécile Feuillie, Wim Jonckheere, Claire Valotteau, Yves F. Dufrêne, and Han Remaut. "Nucleation and growth of a bacterial functional amyloid at single-fiber resolution." *Nature chemical biology* 13, no. 8 (2017): 902-908.

Snitkin, Evan S., Adrian M. Zelazny, Pamela J. Thomas, Frida Stock, NISC Comparative Sequencing Program, David K. Henderson, Tara N. Palmore, and Julia A. Segre. "Tracking a hospital outbreak of carbapenem-resistant Klebsiella pneumoniae with whole-genome sequencing." *Science translational medicine* 4, no. 148 (2012): 148ra116-148ra116.

Song, Qinghe, Junjun Liu, Liyuan Dong, Xiaolei Wang, and Xiandang Zhang. "Novel advances in inhibiting advanced glycation end product formation using natural compounds." *Biomedicine & Pharmacotherapy* 140 (2021): 111750.

Strom, A. R., and I. Kaasen. "Trehalose metabolism in Escherichia coli: stress protection and stress regulation of gene expression." *Molecular microbiology* 8, no. 2 (1993): 205-210.

Tinnirello, Rosaria, Gioacchin Iannolo, Alberto Cagigi, and Bruno Douradinha. "An overview of Klebsiella pneumoniae ST392 amid the AMR silent pandemic and consequent environmental dissemination and health risks." *International Journal of Hygiene and Environmental Health* 271 (2026): 114710.

Twarda-Clapa, Aleksandra, Aleksandra Olczak, Aneta M. Białkowska, and Maria Koziołkiewicz. "Advanced glycation end-products (AGEs): formation, chemistry, classification, receptors, and diseases related to AGEs." *Cells* 11, no. 8 (2022): 1312.

Vanaporn, Muthita, and Richard W. Titball. "Trehalose and bacterial virulence." *Virulence* 11, no. 1 (2020): 1192-1202.

Wang, Xun, Cody G. Cole, Cory D. DuPai, and Bryan W. Davies. "Protein aggregation is associated with Acinetobacter baumannii desiccation tolerance." *Microorganisms* 8, no. 3 (2020): 343.

Winkler, Juliane, Anja Seybert, Lars König, Sabine Pruggnaller, Uta Haselmann, Victor Sourjik, Matthias Weiss, Achilleas S. Frangakis, Axel Mogk, and Bernd Bukau. "Quantitative and spatio-temporal features of protein aggregation in Escherichia coli and consequences on protein quality control and cellular ageing." *The EMBO journal* 29, no. 5 (2010): 910-923.

Wood, Janet M. "Bacterial responses to osmotic challenges." *The Journal of general physiology* 145, no. 5 (2015): 381.

Wu, Josephine W., Kuan-Nan Liu, Su-Chun How, Wei-An Chen, Chia-Min Lai, Hwai-Shen Liu, Chaur-Jong Hu, and Steven S-S. Wang. "Carnosine's effect on amyloid fibril formation and induced cytotoxicity of lysozyme." *PloS one* 8, no. 12 (2013): e81982.

Zheng, Qingfei, Nathaniel D. Omans, Rachel Leicher, Adewola Osunsade, Albert S. Agustinus, Efrat Finkin-Groner, Hannah D'Ambrosio et al. "Reversible histone glycation is associated with disease-related changes in chromatin architecture." *Nature communications* 10, no. 1 (2019): 1289.